Annals of R.S.C.B., ISSN:1583-6258, Vol. 25, Issue 5, 2021, Pages. 1587 - 1628
Received 15 April 2021; Accepted 05 May 2021.

Molecular Docking, Vibrational, Structural and Electronic Studies of 5-(4-Butoxybenzylidene)-2-[3-(4-Chlorophenyl)-5[4-(Propan-2-Yl)-4,5-Dihydro-1H-Pyrazol-1-Yl]-1,3-Thiazol-4(5H)-One

K.Venil[a], A.Lakshmi[a] , V. Balachandran[b]

[a] Department of Physics, Government Arts College (Affiliated to Bharathidasan University), Trichy 621 222, TN, India.

[b]Centre for Research, Department of Physics, Arignar Anna Government Arts College, Musiri ,621 211, TN, India

Abstract

Spectroscopic and structural investigations of 5-(4-Butoxybenzylidene)-2-[3-(4-chlorophenyl)-5[4-(propan-2-yl)-4, 5-dihydro-1H-pyrazol-1-yl]-1,3-thiazol-4(5H)-one are presented by using experimental (FT-IR and FT-Raman) spectra and theoretical (Density functional theory) calculations. The optimized geometrical assignments were made on the basis of potential energy distribution. The molecular electrostatic potential map was used to detect the electrophilic and nucleophilic sites in the molecule. The directly calculated ionization potential (I), electron affinity (A), electronegativity (χ), electrophilic index (ω), hardness (η) and chemical potential (μ) are all correlated from HOMO-LUMO energies with their molecular properties. The reduced density gradient of the title molecule was investigated by the interaction of molecule. Molecular docking studies were also described.

Keywords:DFT, Thiazole, Reduced Density Gradient and Docking.

1. Introduction

Thiazoleis a heterocyclic compound that contains both sulphur and nitrogen and a large family of derivatives. Thiazole itself is a pale yellow liquid with a pyridine-like odor and they have extensive applications in agriculture and medicinal chemistry [1, 2]. Varieties of biologically active molecules accommodate the thiazole and its derivatives, aminothiazoles [3]. They are used as important fragments in different drugs related to anti-tuberculosis, anti-inflammatory, [4, 5, 6], anti-allergic [7], anti-hypertensive [8], schizophrenia [9], anti-bacterial, HIV infections [4, 10] and human

Annals of R.S.C.B., ISSN:1583-6258, Vol. 25, Issue 5, 2021, Pages. 1587 - 1628
Received 15 April 2021; Accepted 05 May 2021.

lymphatic filarial parasites [11]. Various thiazole derivatives are used as fungicides and herbicides and have numerous applications in agricultural field [12]. Hydantoin derivatives, in particular phenytoin, are important antiepileptic drugs.

In the present work, optimized molecular structure of the title compound is investigated. The vibrational spectroscopic investigations combined with DFT (Density functional theory)calculations are employed to provide comprehensive vibrational spectral assignments of the title compound. The molecular properties like dipole moment, polarizability, hyper polarizability and molecular electrostatic potential surface have been calculated to get a better understanding the properties of the title molecule.The non-covalent interactions like hydrogen bonding and Van der Waals interaction were identified from the molecular geometry and electron localization function. These interactions in molecules have been studied by using reduced density gradient (RDG) and graphed by Multiwfn.Molecular docking is a computer-assisted drug design (CADD) method used to predict the favourable orientation of a ligand (viz. drug) to a target (viz. receptor) when bound to each other to form a stable complex.

2. Experimental details

5-(4-Butoxybenzylidene)-2-[3-(4-chlorophenyl)-5[4-(propan-2-yl)-4, 5-dihydro-1H-pyrazol-1-yl]-1,3-thiazol-4(5H)-one was synthesized as per the reported procedure [13-15]. The Fourier Transform infrared (FT-IR) spectrum of the title compound was recorded using Perkin Elmer Spectrometer fitted with a KBr beam splitter around 4000-450 cm^{-1}. The Bruker RFS 27 FT-Raman spectrometer in the region 4000-0 cm^{-1} using a 1064 nm Nd:YAG laser source was used to reported the FT-Raman spectrum. Both the spectral measurements were performed at the Sophisticated Analytical Instrumentation Facility (SAIF), IIT, Madras, India.

3. Computational details

All calculations of the title compound were carried out using Gaussian 09 program [16] was performed with Becke's three-parameter hybrid model and therefore the Lee-Yang-Parr correlation was a useful functional (B3LYP) in DFT [17, 18] technique. The electronic structure of the molecule has to be proven with the density functional theory. The visual representations for fundamental modes are also checked by the Gauss view program [19]. Electron density map and reduced density

Annals of R.S.C.B., ISSN:1583-6258, Vol. 25, Issue 5, 2021, Pages. 1587 - 1628
Received 15 April 2021; Accepted 05 May 2021.

gradient (RDG) were calculated with the use of Multiwfn program [20] and plotted by visual molecule dynamics program (VMD) [21]. The reactivity descriptors, such as electrophilicity (ω), global hardness (η), the chemical potential (μ), ionization potential (I) and electron affinity (A) were determined from the energies of frontier molecular orbitals. The molecular docking calculation was performed by the AutoDock 4.0.1 software [22], which was also applied to detect the docking input files and analyze the docking result. Using Discovery studio visualize software, one of the best active site was visualized for ligand-protein interaction.

4.0 Results and discussions

4.1 Optimized molecular geometrical parameters

The geometrical structure and parameters of 5-(4-Butoxybenzylidene)-2-[3-(4-chlorophenyl)-5[4-(propan-2-yl)-4,5-dihydro-1H-pyrazol-1-yl]-1,3-thiazol-4(5H)-one are depicted in Figure 1 and Table 1 by using B3LYP/6-31G and B3LYP/6-31G (d,p) methods.

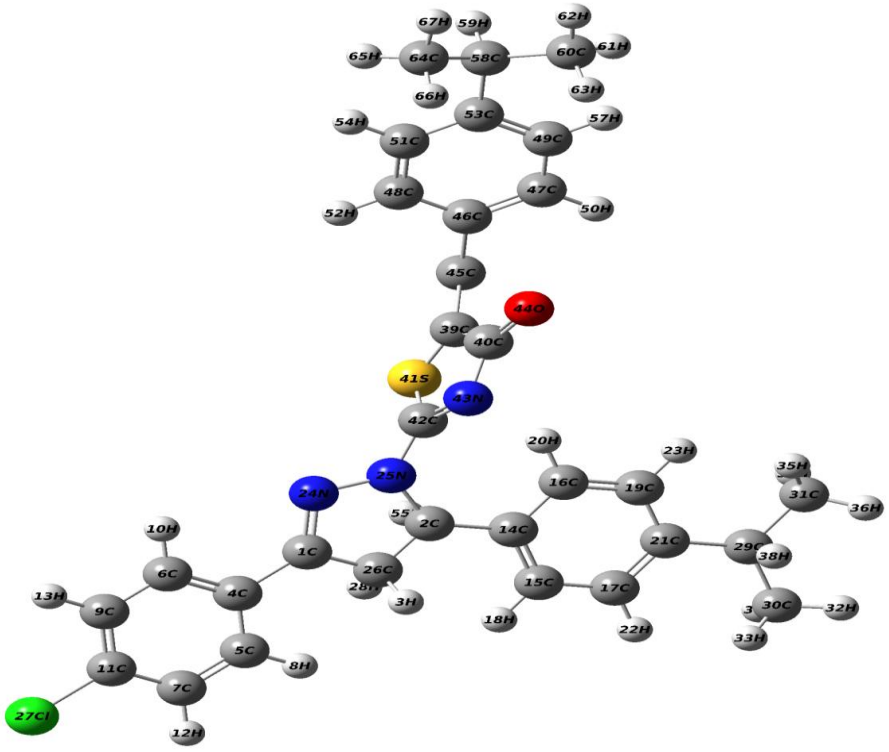

Figure 1: Optimized molecular structure of 5-(4-Propan-2-yl)benzylidene)-2-[3-(4-chlorophenyl)-5[4-(propan-2-yl)phenyl-4,5-dihydro-1H-pyrazol-1-yl]-1,3-thiazol-4(5H)-one

Annals of R.S.C.B., ISSN:1583-6258, Vol. 25, Issue 5, 2021, Pages. 1587 - 1628
Received 15 April 2021; Accepted 05 May 2021.

Table 1: Optimized structural parameters of 5-(4-Butoxybenzylidene)-2-[3-(4-chlorophenyl)-5[4-(propan-2-yl)-4,5-dihydro-1H-pyrazol-1-yl]-1,3-thiazol-4(5H)-one obtained by B3LYP/6-31G and B3LYP/6-31G (d,p) basis sets.

	Bond length (Å)			Bond angle(°)			Dihedral angle(°)	
Parameters	B3LYP/6-31G	B3LYP/6-31G(D,P)	Parameters	B3LYP/6-31G	B3LYP/6-31G(d,p)	Parameters	B3LYP/6-31G	B3LYP/6-31G(D,P)
C1-C4	1.4604	1.4628	C4-C1-N24	121.7147	121.788	N24-C1-C4-C5	179.171	178.663
C1-N24	1.3062	1.294	C4-C1-C26	125.171	125.091	N24-C1-C4-C6	-0.574	-1.023
C1-C26	1.5223	1.5184	N24-C1-C26	113.104	113.11	C26-C1-C4-C5	0.425	-0.056
C1-C14	1.5184	1.5174	C14-C2-N25	112.3446	112.421	C26-C1-C4-C6	-179.319	-179.743
C2-N25	1.5078	1.4931	C14-C2-C26	115.1468	114.938	C4-C1-N24-N25	-179.833	179.898
C2-C26	1.5576	1.5519	C14-C2-N25	109.2771	109.088	C26-C1-N24-N25	-0.948	-1.241
C2-H55	1.0919	1.0919	N25-C2-C26	100.1893	100.201	C4-C1-N26-C2	-174.604	-174.939
H3-C26	1.0937	1.0932	N25-C2-H55	107.2673	107.668	C4-C1-C26-H3	-54.509	-54.804
C4-C5	1.4082	1.4042	C26-C2-H55	121.7147	121.788	C4-C1-C26-H28	65.533	65.160
C4-C6	1.4121	1.4083	C1-C4-C5	125.171	125.091	N24-C1-C26-C2	6.557	6.245
C5-C7	1.3979	1.3933	C1-C4-C6	113.104	113.11	N24-C1-C26-H3	126.652	126.379
C5-C8	1.0844	1.0852	C5-C4-C6	112.3446	112.421	N24-C1-C26-H28	-113.306	-113.657
C6-C9	1.3932	1.3882	C4-C5-C7	115.1468	114.9386	N25-C2-C14-C15	68.304	64.354

Annals of R.S.C.B., ISSN:1583-6258, Vol. 25, Issue 5, 2021, Pages. 1587 - 1628
Received 15 April 2021; Accepted 05 May 2021.

C6-H10	1.0835	1.0843	C4-C5-H8	109.2771	109.088	N25-C2-C14-C16	-111.460	-115.788
C7-C11	1.392	1.3929	C7-C5-H8	100.1893	100.201	C26-C2-C14-C15	-45.540	-49.422
C7-H12	1.0829	1.084	C4-C6-C9	107.2673	107.668	C26-C2-C14-C16	134.697	130.437
C9-C11	1.3963	1.3978	C4-C6-H10	121.7147	121.788	H55-C2-C14-C15	-172.766	-176.292
C9-H13	1.083	1.0842	C9-C6-H10	125.171	125.091	H55-C2-C14-C16	7.471	3.566
C11-Cl27	1.8237	1.7554	C5-C7-C11	113.104	113.11	C14-C2-N25-N24	-113.650	-114.317
C14-C15	1.4058	1.4019	C5-C7-H12	112.3446	112.421	C14-C2-N25-C42	69.525	71.318
C14-C16	1.4006	1.3959	C11-C7-H12	115.1468	114.938	C26-C2-N25-N24	9.079	8.210
C15-C17	1.3957	1.3917	C6-C9-C11	109.2771	109.088	C26-C2-N25-C42	-167.745	-166.155
C15-H18	1.0867	1.0872	C6-C9-H13	100.1893	100.201	H55-C2-N25-N24	126.247	125.504
C16-C19	1.3982	1.3951	C11-C9-H13	107.2673	107.668	H55-C2-N25-C42	-50.578	-48.861
C16-H20	1.0849	1.0859	C7-C11-C9	121.7147	121.788	C14-C2-C26-C1	112.154	112.861
C17-C21	1.4076	1.4037	C7-C11-Cl27	125.171	125.091	C14-C2-C26-C3	-8.727	-7.907
C17-C22	1.086	1.0865	C9-C11-Cl27	113.104	113.11	C14-C2-C26-H28	-128.840	-128.348
C19-C21	1.4035	1.399	C2-C14-C15	112.3446	112.421	N25-C2-C26-C1	-8.582	-7.874
C19-H23	1.0862	1.087	C2-C14-C16	115.1468	114.939	N25-C2-C26-C3	-129.463	-128.642

Annals of R.S.C.B., ISSN:1583-6258, Vol. 25, Issue 5, 2021, Pages. 1587 - 1628
Received 15 April 2021; Accepted 05 May 2021.

C21-C29	1.5261	1.5226	C15-C14-C16	109.2771	109.088	N25-C2-C26-H28	110.424	110.917
N24-N25	1.3915	1.37	C14-C15-C17	100.1893	100.201	H55-C2-C26-C1	-122.075	-121.822
N25-C42	1.3483	1.3513	C14-C15-H18	107.2673	107.668	H55-C2-C26-C3	117.044	117.409
C26-H28	1.0969	1.096	C17-C15-H18	121.7147	121.788	H55-C2-C26-H28	-3.069	-3.032
C29-C30	1.5465	1.5402	C14-C16-C19	125.171	125.091	C1-C4-C5-C7	-179.695	-179.612
C29-C30	1.546	1.5402	C14-C16-H20	113.104	113.11	C1-C4-C5-H8	0.260	0.318
C29-H38	1.0993	1.0978	C19-C16-H20	112.3446	112.421	C6-C4-C5-C7	0.054	0.082
C30-H32	1.0965	1.0953	C15-C17-C21	115.1468	114.938	C6-C4-C5-C8	-179.991	-179.988
C30-H33	1.0953	1.094	C15-C17-H22	109.2771	109.088	C1-C4-C6-C9	179.712	179.627
C30-H34	1.0968	1.0955	C21-C17-H22	100.1893	100.201	C1-C4-C6-H10	-0.241	-0.339
C31-H35	1.0956	1.0944	C16-C19-C21	107.2673	107.668	C5-C4-C6-C9	-0.037	-0.066
C31-H36	1.0966	1.0954	C16-C19-H23	121.7147	121.788	C5-C4-C6-H10	-179.990	179.968
C31-H37	1.0968	1.0956	C21-C19-H23	125.171	125.091	C4-C5-C7-C11	-0.039	-0.047
C39-C40	1.493	1.5081	C17-C21-C19	113.104	113.11	C4-C5-C7-H12	179.976	179.971
C39-S41	1.8656	1.794	C17-C21-C29	112.3446	112.421	H8-C5-C7-C11	-179.994	-179.978
C39-C45	1.3602	1.3596	C19-C21-C29	115.1468	114.939	H8-C5-C7-H12	0.020	0.040

Annals of R.S.C.B., ISSN:1583-6258, Vol. 25, Issue 5, 2021, Pages. 1587 - 1628
Received 15 April 2021; Accepted 05 May 2021.

C40-N43	1.4066	1.3966	C1-N24-N25	109.2771	109.088	C4-C6-C9-C11	0.006	0.015
C40-O44	1.2485	1.2232	C2-N25-N24	100.1893	100.201	C4-C6-C9-H13	-179.979	-179.983
S41-C42	1.8391	1.776	C2-N25-C42	107.2673	107.668	H10-C6-C9-C11	179.958	179.981
C42-N43	1.3043	1.2987	N24-N25-C42	121.7147	121.788	H10-C6-C9-H13	-0.027	-0.018
C45-C46	1.4585	1.4571	C1-C26-C2	125.171	125.091	C5-C7-C11-C9	0.006	-0.006
C45-C56	1.0902	1.0904	C1-C26-H3	113.104	113.11	C5-C7-C11-Cl27	-179.973	-179.967
C46-C47	1.416	1.4105	C1-C26-H28	112.3446	112.421	H12-C7-C11-C9	179.992	179.977
C46-C48	1.4198	1.4156	C2-C26-H3	115.1468	114.939	H12-C7-C11-Cl27	0.013	0.016
C47-C49	1.3931	1.3906	C2-C26-H28	109.2771	109.088	C6-C9-C11-C7	0.010	0.021
C47-H50	1.0867	1.0872	H3-C26-H28	100.1893	100.201	C6-C9-C11-Cl27	179.989	179.982
C48-C51	1.3882	1.3839	C21-C29-C30	107.2673	107.668	H13-C9-C11-C7	179.995	-179.980
C48-H52	1.0817	1.082	C21-C29-C31	121.7147	121.788	H13-C9-C11-Cl27	-0.026	-0.019
C49-C53	1.4036	1.4017	C21-C29-H38	125.171	125.091	C2-C14-C15-C17	179.751	179.385
C49-H57	1.0828	1.0831	C30-C29-C31	113.104	113.11	C2-C14-C15-H18	-0.979	-1.326
C51-C53	1.4054	1.4049	C30-C29-H38	112.3446	112.421	C16-C14-C15-C17	-0.483	-0.476
C51-H54	1.0837	1.0851	C31-C29-H38	115.1468	114.939	C16-C14-C15-H18	178.787	178.813

Annals of R.S.C.B., ISSN:1583-6258, Vol. 25, Issue 5, 2021, Pages. 1587 - 1628
Received 15 April 2021; Accepted 05 May 2021.

C53-O58	1.3842	1.3595	C29-C30-H32	109.2771	109.088	C2-C14-C15-C19	-179.424	-179.063
O58-C59	1.4618	1.4285	C29-C30-H33	100.1893	100.201	C2-C14-C16-H20	2.293	2.184
C59-H60	1.0988	1.0996	C29-C30-H34	107.267	107.668	C15-C14-C16-C19	0.806	0.799
C59-H61	1.0988	1.0996	C40-C39-C45	113.104	113.11	C15-C14-C16-H20	-177.477	-177.954
C59-C62	1.5233	1.5217	S41-C39-C45	118.135	118.670	C14-C15-C17-C21	-0.126	-0.137
C62-H63	1.0976	1.0969	C39-C40-N43	113.471	112.705	C14-C15-C17-H22	179.731	179.737
C62-H64	1.0976	1.0969	C39-C40-O44	124.813	124.954	H18-C15-C17-C21	-179.403	-179.432
C62-C65	1.5402	1.5336	N43-C40-O44	121.716	122.339	H18-C15-C17-H22	0.454	0.442
C65-H66	1.1	1.0984	C39-S41-C42	86.313	87.757	C14-C16-C19-C21	-0.532	-0.522
C65-H67	1.1	1.0984	N25-C42-S41	119.688	119.294	C14-C16-C19-H23	-179.815	-179.889
C65-C68	1.5369	1.5315	N25-C42-N43	122.861	122.033	H20-C16-C19-C21	177.745	178.228
C68-H69	1.0969	1.0956	S41-C42-N43	117.447	118.672	H20-C16-C19-H23	-1.538	-1.139
C68-H70	1.0958	1.0945	C40-N43-C42	113.818	112.104	C15-C17-C21-C19	0.407	0.421
C68-H71	1.0969	1.0956	S41-C39-C45	118.135	118.670	C15-C17-C21-C29	179.921	-179.872

For the title compound, the C-C bond length for pyrazole ring of C1-C26, C2-C26 are 1.5223/1.5184, 1.5576/1.5519 Å, for thiazole ring for C39-C40 is 1.493/1.5081 Å for the B3LYP/6-31G and B3LYP/6-31G (d,p) methods and these values are in between the single and double bond (1.54 Å and 1.33 Å) [23]. In the present work, the C-O bond length are observed at

Annals of R.S.C.B., ISSN:1583-6258, Vol. 25, Issue 5, 2021, Pages. 1587 - 1628
Received 15 April 2021; Accepted 05 May 2021.

C40-O44=1.2485/1.2232 Å, C53-O58 = 1.3842 / 1.3595Å, O58-C59=1.4618/1.4285Å which are in good agreement with the reported values for a similar derivatives (1.3871 Ǻ and 1.3653 Ǻ) [24]. The C-N bond length for the title compound are C1-N24, C2-N25, N25-C42, C40-N43, C42-N43 are 1.3062/1.294 Å, 1.5078/1.4931 Å, 1.3483/1.3513 Å, 1.4066/1.3966 Å, 1.3043/1.2987 Å which are in agreement with the literature [25]. The C-S bond length for the title compoundare 1.8656/1.794 Å for C39-S41 and for S41-C42 is 1.8656/1.794 Å, 1.8391 /1.776 Å and is similar toKuruvilla et.al [26] observed the C-S value at C5-S9= 1.748 Å and C8-S9=1.733 Å theoretically and experimentally at 1.8642, 1.862 Å. In the case of C-H bond lengths, (DFT/XRD) it is observed that aromatic C-H bonds measure 1.10/1.09 Å, which is equal to the experimental value. For the title compound, the bond lengths for C2-H55, C6-H10, C9-H13,C31-H35, C47-H50, C65-H66, C68-H70, C68-H71 are 1.0919/1.0919, 1.0835/1.0843, 1.083/1.0842, 1.0956/1.0944, 1.0867/1.0872, 1.1/1.0984, 1.0958/1.0945 and 1.0969/1.0956 Å observed. It was also very confined to experimental value [27]. The N-N bond lengths (DFT/XRD) are reported in the range 1.3409-1.3886Ǻ [28] and in the present case (BPT1), the N-N bond length is found at 1.3915/1.37 Ǻ for N24-N25. The thiazole ring is tilted from the phenyl ring as is evident from the torsion angles C45-C39-C40-N43=179.99/179.97˚, S41-C39-C40-H43 = -0.1457/-0.2921˚, C40-C39-S41-C42= 0.3713/ 0.414˚ and C45-C39-S41-C42= -179.74/-179.81˚.

For the title compound, the interactions between the thiazole and pyrazole groups are C40-C39-C45 = 132.917/132.571, S41-C39-C45 = 118.135/118.669, C39-C40-N43 = 113.471 /112.705, C39-C40-O44 = 124.813 / 124.954, N43-C40-O44 = 121.716/ 122.339, C39-S41-C42 = 86.313/87.757, N25-C42-S41= 119.688/119.294, N25-C42-N43 = 122.861 / 122.033, S41-C42-N43 = 117.447/118.672, C40-N43-C42 = 113.818 / 112.104 respectively.

4.2 Vibrational assignments

The title compound is consist of 71 atoms and has 207 fundamental modes of vibrations. The observed and simulated FT-IR and FT-Raman spectra of 5-(4-Butoxybenzylidene)-2-[3-(4-chlorophenyl)-5[4-(propan-2-yl)-4,5-dihydro-1H-pyrazol-1-yl]-1,3-thiazol-4(5H)-one at B3LYP level using 6-31G and 6-31G(d,p) basis sets are shown in Figures 2 and 3. The elaborated vibrational assignments of the title compound along with the calculated IR and Raman frequencies and normal mode descriptions are given in Table 2.

Annals of R.S.C.B., ISSN:1583-6258, Vol. 25, Issue 5, 2021, Pages. 1587 - 1628
Received 15 April 2021; Accepted 05 May 2021.

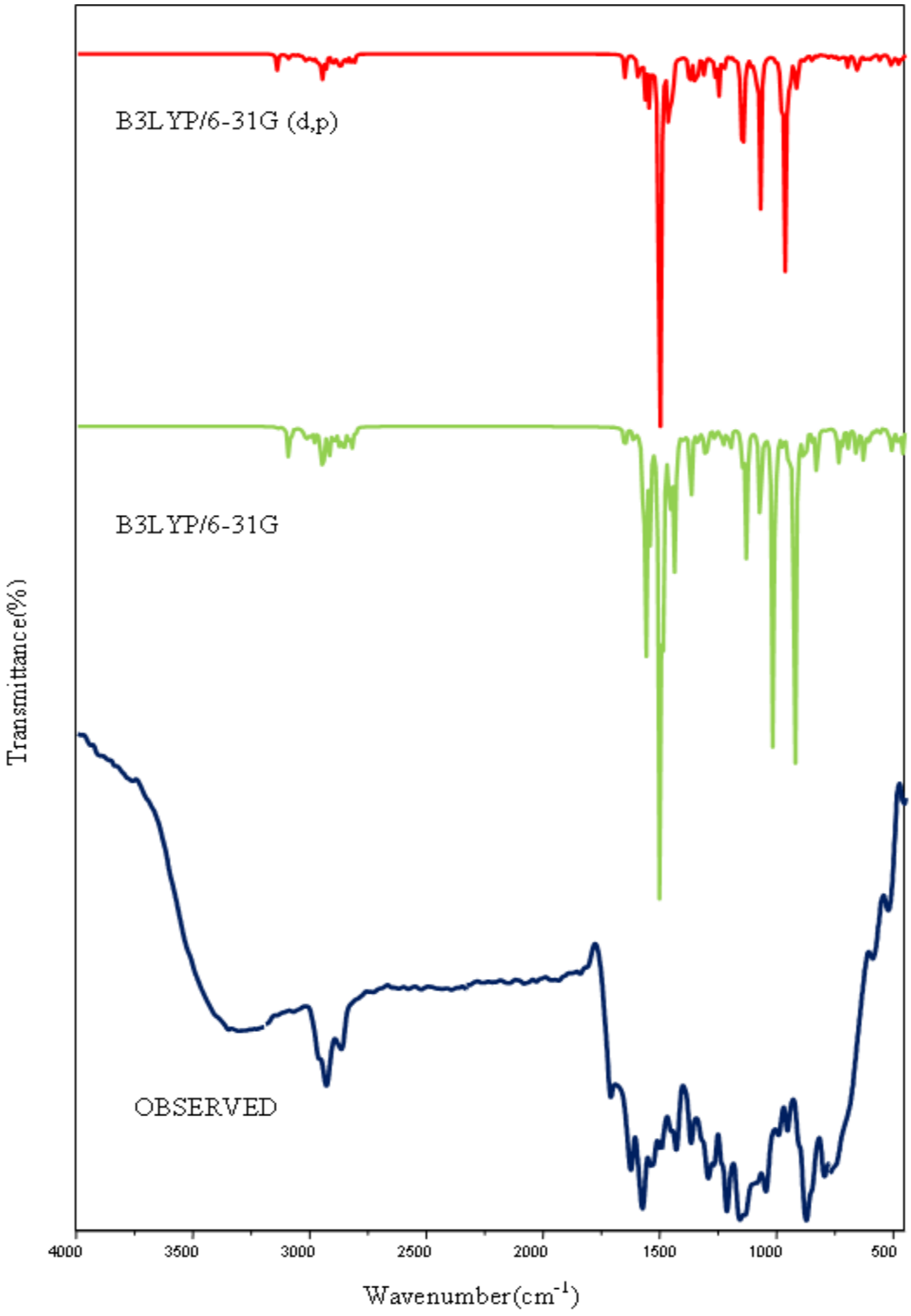

Figure 2:Observed FT-IR and simulated spectra of 5-(4-Butoxybenzylidene)-2-[3-(4-chlorophenyl)-5[4-(propan-2-yl)-4,5-dihydro-1H-pyrazol-1-yl]-1,3-thiazol-4(5H)-one

Annals of R.S.C.B., ISSN:1583-6258, Vol. 25, Issue 5, 2021, Pages. 1587 - 1628
Received 15 April 2021; Accepted 05 May 2021.

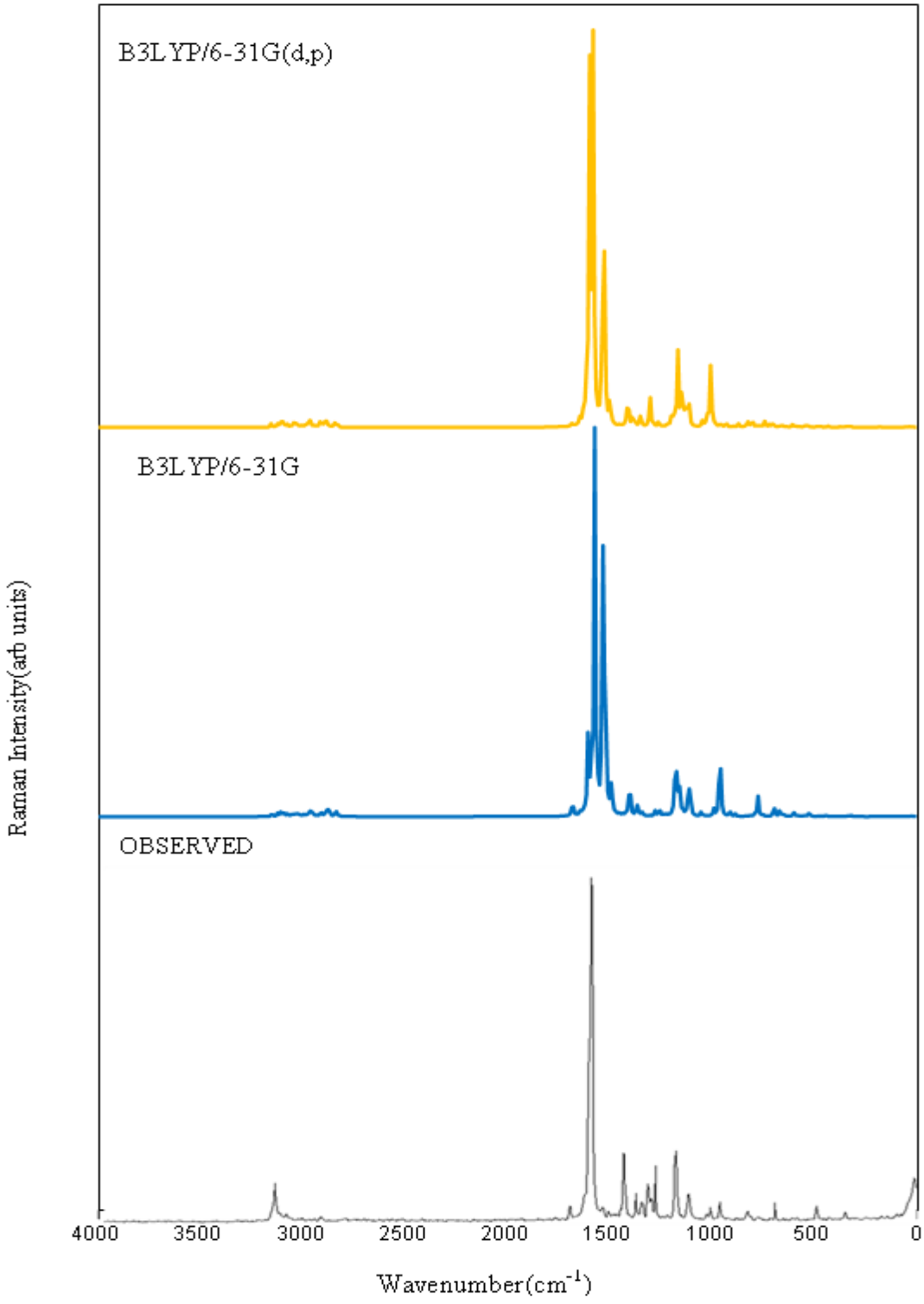

Figure 3:Observed FT-Raman and simulated spectra of 5-(4-Butoxybenzylidene)-2-[3-(4-chlorophenyl)-5[4-(propan-2-yl)-4,5-dihydro-1H-pyrazol-1-yl]-1,3-thiazol-4(5H)-one

Annals of R.S.C.B., ISSN:1583-6258, Vol. 25, Issue 5, 2021, Pages. 1587 - 1628
Received 15 April 2021; Accepted 05 May 2021.

Table 2:Vibrational assignments of 5-(4-Butoxybenzylidene)-2-[3-(4-chlorophenyl)-5[4-(propan-2-yl)-4,5-dihydro-1H-pyrazol-1-yl]-1,3-thiazol-4(5H)-one one by B3LYP/6-31G and B3LYP/6-31G (d,p) basis sets.

Modes	Observed wavenumbers (cm^{-1})		Calculated wavenumbers(cm^{-1})		Vibrational assignments
	FT-IR	FT-Raman	B3LYP/6-31G	B3LYP/6-31G(d,p)	
1		3150	3156	3152	υCH(98)
2			3125	3123	υCH(98)
3			3110	3107	υCH(98)
4			3099	3095	υCH(98)
5			3094	3088	υCH(98)
6		3075	3078	3074	υCH(98)
7			3058	3055	υCH(98)
8			3045	3043	υCH(98)
9			3038	3034	υCH(98)
10			3033	3029	υCH(98)
11			3026	3021	υCH(98)
12			3016	3011	υCH(98)
13		3002	3010	3003	υCH(98)
14			3001	2995	υassCH_3(96)
15			2986	2983	υassCH_3(97)
16			2976	2971	υassCH_3(97)
17			2970	2966	υassCH_2(95)
18			2964	2959	υassCH_3(96)
19			2950	2947	υassCH_3(97)
20			2936	2935	υCH(98)

Annals of R.S.C.B., ISSN:1583-6258, Vol. 25, Issue 5, 2021, Pages. 1587 - 1628
Received 15 April 2021; Accepted 05 May 2021.

21	2922		2930	2926	υassCH$_3$(98)
22			2922	2919	υassCH$_2$(96)
23		2910	2915	2912	υssCH$_2$ (96)
24			2910	2906	υassCH$_2$ (97)
25			2896	2893	υssCH$_2$ (96)
26			2888	2884	υssCH$_3$(97)
27			2882	2878	υssCH$_3$ (96)
28			2872	2869	υassCH$_2$ (97)
29	2856		2860	2854	υssCH$_3$ (96)
30			2846	2843	υCH(98)
31			2841	2835	υssCH$_2$ (96)
32			2830	2822	υssCH$_2$ (96)
33	1679	1680	1683	1680	υCO(72), υCC(20)
34			1644	1641	υCC(70), δCH(18)
35			1625	1623	υCC(71), δCH(20)
36			1613	1604	υCC(70), δCH(22)
37	1591		1596	1590	υCC(68), υCN(12), δCH(10)
38			1579	1572	υCN(65), υCC(14), δCH(10)
39			1563	1559	υCC(64), δCH(14), δCC(11)
40			1538	1533	υCC(60), δCCl(18), υCN(10)
41	1541		1533	1529	υCN(65), υCC(15), δCH(12)
42			1525	1517	υCN(65), υCC(16), δCH(12)
43	1506	1510	1512	1508	δCH(64), υCC(18)

Annals of R.S.C.B., ISSN:1583-6258, Vol. 25, Issue 5, 2021, Pages. 1587 - 1628
Received 15 April 2021; Accepted 05 May 2021.

44			1499	1493	δCH(64), υCC(20)
45	1485	1485	1490	1486	δCH(65), υCC(18)
46			1481	1475	δ_{opb} CH_3 (72)
47			1477	1470	δ_{opb} CH_3(75)
48			1472	1466	δ_{opb} CH_3(73)
49			1455	1451	δ_{ipb} CH_3(73)
50			1442	1436	δ_{ipb} CH_3(72)
51			1437	1430	δ_{ipb} CH_3(72)
52			1429	1422	σ_{sci} CH_2(80)
53		1415	1423	1415	σ_{sci} CH_2(80)
54			1420	1408	δCH(65), υCC(21)
55			1414	1403	δCH(66), υCC(22)
56		1400	1408	1399	σsci CH_2(80)
57	1394		1402	1395	σsci CH_2(81)
58			1388	1383	δsb CH_3(75)
59			1385	1379	δsb CH_3(75)
60			1376	1370	δsb CH_3(74)
61			1370	1362	υCN(64)
62		1350	1356	1351	υCN(65), δCH(14)
63			1346	1342	δCO(67)
64	1329		1335	1330	δCH(67)
65			1327	1323	δCH(68)
66		1310	1318	1312	δCH(66), υCC(14)
67			1308	1302	δCH(66), υCC(15)
68		1295	1301	1297	υCO(66), δCH(12)
69		1280	1285	1281	δCH(66), υCC(12)

Annals of R.S.C.B., ISSN:1583-6258, Vol. 25, Issue 5, 2021, Pages. 1587 - 1628
Received 15 April 2021; Accepted 05 May 2021.

70			1278	1275	δCH(66), υCC(12), υCN(10)
71			1266	1263	δCH(64), υCN(18), υCC(10)
72	1254	1250	1260	1254	υCO(65), δCH(17), υCcl(10)
73			1248	1244	δCH(66), υCC(12), υCN(10)
74	1230		1236	1231	υCC(63), δCH(16), υCN(12)
75		1215	1221	1217	υCC(65), δCH(18)
76			1214	1207	ρrockCH_2(70), δCH(12)
77		1200	1210	1200	ρrockCH_2(70), δCH(12)
78			1195	1191	υCC(65), δCH(14)
79			1186	1182	υCC(66), δCH(15)
80	1173		1179	1175	ρrockCH_2(70)
81			1165	1163	ρrockCH_2(69)
82			1162	1158	υCC(68)
83			1145	1143	υCC(68)
84			1140	1136	υCC(68)
85			1131	1127	υCC(66)
86	1118		1125	1120	υCC(66)
87			1118	1113	τCH_2(75)
88			1110	1105	τCH_2(75)
89			1102	1097	γCH(60)
90			1093	1088	γCH(60)
91			1080	1075	υCC(65), δCH(13)
92			1056	1051	τCH_2(75)

Annals of R.S.C.B., ISSN:1583-6258, Vol. 25, Issue 5, 2021, Pages. 1587 - 1628
Received 15 April 2021; Accepted 05 May 2021.

93			1044	1040	τCH_2(74)
94			1032	1028	γopr CH_3(62), υCC(10)
95			1021	1017	γopr CH_3(63), υCC(10)
96			1013	1009	υCC(74), υCO(16)
97	1002		1003	1000	γopr CH_3(64)
98			992	989	υCC(66), δCH(15)
99			984	980	δCO(66), δCH(14)
100			965	963	δCO(65), δCH(12)
101			960	956	γCH(58), γ_{ring}(26)
102	948	950	953	948	γCH(58), γ_{ring}(26)
103			935	933	γCH(58), γ_{ring}(25)
104			932	929	γCH(58), γ_{ring}(21)
105			925	921	υCC(72), υCO(15), δCH(10)
106			924	916	υCC(63), δCH(18)
107	909	910	914	910	υCC(64), δCH(20)
108			889	885	γCH(58), γ_{ring}(18)
109			883	879	υNN(65), δCH(18)
110			867	865	γCH(55), γCC(18)
111			845	842	γCC(18), δwagg CH_2(12)
112			840	834	γCH(62), γ_{ring}(18)
113	827		833	829	γCH(58), γCC(21)
114			823	820	γCH(58), γCC(20)
115			817	812	δ_{wagg} CH_2(58), γCC(20)
116		800	805	802	δ_{wagg} CH_2(58), γCC(21)
117			800	795	γCH(56), γCC(18)

Annals of R.S.C.B., ISSN:1583-6258, Vol. 25, Issue 5, 2021, Pages. 1587 - 1628
Received 15 April 2021; Accepted 05 May 2021.

118			796	790	γCH(55), γCC(17)
119			792	786	δCC(63), δCH(18)
120			785	780	δ_{wagg} CH_2(57)
121			779	773	γCH(58), γ_{ring}(18)
122			775	769	δ_{wagg} CH_2(58), γCC(20)
123			768	765	δ_{ipr} CH_3(68)
124			760	756	δ_{ipr} CH_3(68)
125	747		741	748	δ_{ipr} CH_3(68)
126			738	731	υCS(74), δCH(20)
127		720	726	720	υCN(64), υCC(16)
128			715	711	δCC(60), δ_{ipr} CH_3(19)
129			706	700	γCH(58), γ_{ring}(16)
130			697	694	υCS(75), δCH(20)
131			690	688	δCC(60), δ_{ipr}(17)
132			685	679	γCO(58)
133			670	666	γCC(68)
134			664	659	γCC(68)
135			658	655	γCC(68)
136			653	648	δ_{ring}(56)
137			646	643	δ_{ring}(56)
138			640	638	δ_{ring}(56)
139			635	631	γCC(66)
140			630	626	γCO(51), γ_{ring}(17)
141			625	620	γCO(50), γ_{ring}(17)
142			616	612	δCC(58)
143			608	603	δCC(59)

Annals of R.S.C.B., ISSN:1583-6258, Vol. 25, Issue 5, 2021, Pages. 1587 - 1628
Received 15 April 2021; Accepted 05 May 2021.

144	597		602	598	υCCl(68), δ_{ring}(25)
145			590	586	δCC(58)
146			588	580	δ_{ring}(52)
147			575	573	δCC(58)
148			565	561	δCC(58)
149	551		553	550	δ_{ring}(52)
150			545	541	δ_{ring}(53)
151			539	535	δCC(59)
152			531	523	δ_{ring}(52)
153			522	518	δ_{ring}(50)
154			510	506	δCC(58)
155	503	502	503	500	δCC(58)
156			487	481	δ_{ring}(54)
157			477	472	δCC(59)
158			480	466	δCC(59)
159	457		463	460	δ_{ring}(55)
160	438		445	440	δCCl(60), δ_{ring}(15)
161			427	422	δ_{ring}(52)
162	411		417	410	δ_{ring}(54)
163			407	401	δ_{ring}(50)
164			392	389	δ_{ring}(52)
165			381	375	δ_{ring}(52)
166			371	366	δCC(53)
167			360	354	δCC(54)
168		345	349	345	δCC(54)
169			337	332	δCC(54)

Annals of R.S.C.B., ISSN:1583-6258, Vol. 25, Issue 5, 2021, Pages. 1587 - 1628
Received 15 April 2021; Accepted 05 May 2021.

170			330	325	γCC(55)
171			319	314	γCC(54)
172			303	299	γCC(53)
173			296	293	γCC(55)
174			291	286	γCC(54)
175			280	275	γCCl(55)
176			273	268	γCC(50)
177			262	259	γCC(54)
178			246	242	γCC(50)
179			230	221	τCH_3(55)
180			218	212	τCH_3(54)
181			210	206	τCH_3(54)
182			197	191	γCC(55)
183			189	185	γCC(55)
184			176	173	γCC(55)
185			166	162	δ_{ring}(58)
186		150	158	151	γCC(55)
187			146	142	δ_{ring}(55)
188		135	141	136	γCC(56)
189			135	128	γ_{ring}(56)
190		120	126	120	γCC(56)
191			112	102	δ_{ring}(53)
192		92	95	89	γ_{ring}(54)
193			86	79	γ_{ring}(53)
194			80	74	γ_{ring}(54)
195			75	69	γ_{ring}(53)

Annals of R.S.C.B., ISSN:1583-6258, Vol. 25, Issue 5, 2021, Pages. 1587 - 1628
Received 15 April 2021; Accepted 05 May 2021.

196			66	57	γ_{ring}(51)
197			60	49	δ_{ring}(58)
198			52	46	δ_{ring}(58)
199			48	43	δ_{ring}(58)
200		35	41	35	γ_{ring}(54)
201			37	30	γ_{ring}(53)
202			30	24	γ_{ring}(54)
203			25	22	γ_{ring}(54)
204			23	20	γ_{ring}(53)
205			17	16	γ_{ring}(54)
206			12	10	γ_{ring}(54)
207			7	6	γ_{ring}(54)

ν-stretching, νsym-sym stretching, νasym-asym stretching, δ-in-plane bending, γ-out-of-plane bending, ρ-scissoring, ω-wagging, σ-rocking, τ-twisting.

4.2.1 C-H vibrations

The substituted aromatic structures show the presence of C-H stretching vibration in the region 3100-3000 cm^{-1} which is the characteristic region for the identification of C-H stretching vibrational modes [29-31].

Soleymani et al [32] observed the C-H vibrations at 3112, 3113 3071, 2978 cm^{-1} theoretically and 3050, 3128 cm^{-1} experimentally. Saruadevi et al [33] reported the C-H stretching modes are observed at 3096 cm^{-1} in the IR spectrum and at 3097, 3063, 3038 cm^{-1} in the Raman spectrum experimentally and at 3098, 3075, 3072, 3066, 3055, 3044 cm^{-1} theoretically. Renjith et al [34] reported the C-H stretching vibrations at 3097, 3086, 3081, 3057, 3055 cm^{-1} in the IR spectrum and 3077, 3064 cm^{-1} in the Raman spectrum. C-H stretching are found at 3090, 3062, 2964, 2940 cm^{-1} in FT-Raman and at 2934, 2771 cm^{-1} in FT-IR by Kuruvilla et.al. [26]. Kuruvilla et.al. [27] observed the C-H vibrations experimentally at 3050, 2900 cm^{-1} in FT-IR spectrum and 3042, 2976, 2891, 2850 cm^{-1} in FT- Raman

Annals of R.S.C.B., ISSN:1583-6258, Vol. 25, Issue 5, 2021, Pages. 1587 - 1628
Received 15 April 2021; Accepted 05 May 2021.

spectrum. For our title molecule, the C-H stretching vibrations observed at 3150, 3075, 3002 cm^{-1} for FT-Raman spectrum, 3156,3125, 3110, 3099, 3094, 3078, 3058, 3045, 3038, 3033, 3026, 3016, 3010, 2936, 2846 cm^{-1} and 3152, 3123, 3107, 3095, 3088, 3074, 3055, 3043, 3034, 3029, 3021, 3011, 3003, 2935,2843 cm^{-1} are calculated by B3LYP method with 6-31G and 6-31G(d,p) basis sets.

Jeyasheela et al [35] observed the C-H in-plane bending vibrations at 1179, 1059 cm^{-1} in Raman spectrum and at 1167, 1086, 1046 cm^{-1} in IR spectrum and computed bands appeared at 1318, 1170, 1094, 1059 cm^{-1}.Tamilelakkiya et al [36] observed the C-H stretching mode at 1543, 1440 cm^{-1} in IR spectrumand 1540, 1477 cm^{-1} in Raman spectrum and was calculated in the range of 1511-1445 cm^{-1}. Saraudevi et al [33] reported the C-H bands theoretically at 1277, 1248, 1170, 1140, 1108, 1102, 1042 cm^{-1} and experimentally observed at 1250, 1114, 1044 cm^{-1} in IR spectrum and 1279, 1246, 1168, 1038 cm^{-1} in Raman spectrum. In our title molecule, the C-H in-plane bending vibrations occurs at 1506, 1485, 1329 and 1510, 1485, 1310, 1280 cm^{-1}observed in FT-IR and FT-Raman spectrum and calculated theoretically at 1512, 1499, 1490, 1420, 1414, 1335, 1327, 1308,1285, 1278, 1266, 1248 and 1508, 1493, 1486, 1475, 1408, 1403, 1330, 1323, 1302, 1281, 1275, 1263, 1244 cm^{-1} for the same basis set.

Saraudevi et al [33] observed the CH out-of-plane bending vibrations theoretically at 930, 897, 895, 858, 818, 811, 731 cm^{-1} and experimentally at 931, 896, 855, 816 for IR, 788, 729 cm^{-1} for Raman spectrum. In the present work, the C-H out-of-plane bending vibrations occurs at 948, 827and 950 for FT-IR and FT-Raman spectrum and calculated theoretically at 960, 953, 935, 932, 889, 840,833, 823,796, 779, 706 and 956, 948, 933, 929, 885, 865, 834, 829, 820, 795, 790, 773,700 by B3LYP/6-31G and B3LYP/6-31G(d,p) respectively.

4.2.2 CH_3 vibrations

The CH_3 modes are occurs in the region 2900-3050 cm^{-1} [37]. Asymmetric and symmetric stretching modes of a methyl group attached to the benzene ring are usually downshifted because of electronic effects and are expected near 2925 and 2865 cm^{-1} for asymmetric and symmetric stretching vibrations[38].

The asymmetric stretching modes of the methyl group are calculated at 3047, 3039, 3022, 3003 cm^{-1} by Paniker et al [39]. For the title compound, asymmetric stretching vibrations observed at 2922 cm^{-1}

Annals of R.S.C.B., ISSN:1583-6258, Vol. 25, Issue 5, 2021, Pages. 1587 - 1628
Received 15 April 2021; Accepted 05 May 2021.

for IR spectrum, theoretically observed at 3001, 2986, 2976, 2964, 2950, 2930 cm^{-1} and 2995, 2983, 2971, 2959, 2947, 2926 $cm^{-1}$by B3LYP/6-31G and B3LYP/6-31G(d,p) respectively.

The symmetric modes are observed at 3038, 2946 cm^{-1} in the IR spectrum and theoretically observed at 2948, 2943 cm^{-1} by Paniker et al [39]. Saraudevi et al [33] reported the CH_3 stretching mode at 3027, 2970, 2908 cm^{-1} and experimentally observed at 3002, 2972, 2970 cm^{-1}. Parveen et.al [24] observed the CH_3 stretching modes are assigned at 3002, 2980, 2958, 2914 cm^{-1} in the IR spectrum, 2960, 2938 cm^{-1} in the Raman spectrum and theoretically occurs in the range 3032-2906 cm^{-1}.Murugavel et al [40] theoretically the C-H stretching modes of methyl group at 3056, 3022, 2984, 2964, 2944, 2917 and 2911 cm^{-1} is the experimental values 3024 and 2943 cm^{-1}. Alphonsa et al [41] reported CH_3 stretching mode for FT-IR spectrum at 2983, 2924 cm^{-1} and for FT-Raman at 2983, 2944, 2923 cm^{-1} and asymmetric and symmetric stretching vibrations observed at 3059, 3053 cm^{-1} for FT-IR, Raman spectrum and theoretically at 3012 cm^{-1}.For the title compound, symmetric stretching vibrations observed at 2856 cm^{-1} for IR spectrum, theoretically observed at 2888, 2882, 2860 cm^{-1} and 2884, 2878, 2854 $cm^{-1}$by B3LYP/6-31G and B3LYP/6-31G(d,p) respectively.

In this work, the CH_3 in-plane bending vibrations theoretically observed at δ_{opb} = 1481, 1477, 1472 cm^{-1}, δ_{ipb}= 1455, 1442, 1437 cm^{-1}, δ_{sb} = 1388, 1385, 1376 cm^{-1}, δ_{ipr} = 768, 760, 741 cm^{-1}, τCH_3 =230, 218, 210 cm^{-1} by B3LYP/6-31G method and δ_{opb} = 1475, 1470, 1466 cm^{-1}, δ_{ipb}= 1436, 1430, 1422 cm^{-1}, δ_{sb} =1383, 1379, 1370 cm^{-1}, δ_{ipb}= 765, 756, 748 cm^{-1}, τ_{CH3} = 221, 212, 206 cm^{-1} by B3LYP/6-31G(d,p) method. For the title compound, the out-of-plane bending vibration occurs at 1002 $cm^{-1}$for FT-IR spectrum. The theoretically predicted values by B3LYP/6-31G γ_{opr} =1032, 1021, 1003 cm^{-1} by B3LYP/6-31G and 1028, 1017, 1000 cm^{-1} by B3LYP/6-31G (d,p) methods.

4.2.3 CH_2 group

The stretching vibrations of the CH_2 group and deformation modes of CH_2 group (scissoring, wagging, twisting and rocking modes) appears in the regions 3000 ± 20, 2900 ± 25, 1450 ± 30, 1330 ± 35, 1245 ± 45, 780 ± 55 cm^{-1} respectively [37, 42,30].

Parveen et.al [24] observed the CH_2 stretching modes at 2923 cm^{-1} in the Raman spectrum and at 2926, 2966 cm^{-1} theoretically. The deformation modes of CH_2 are assigned at 1439, 1295, 1220, 1148 cm^{-1} in the IR spectrum, 1146 cm^{-1} in the Raman spectrum. Murugavel et al [40] the CH_2 stretching

Annals of R.S.C.B., ISSN:1583-6258, Vol. 25, Issue 5, 2021, Pages. 1587 - 1628
Received 15 April 2021; Accepted 05 May 2021.

vibrations are calculated at 2991 cm^{-1} (asymmetric) and 2944 cm^{-1} (symmetric). Asymmetric bending of is found at 1275 cm^{-1} which is consistent with the DFT value of 1274 cm^{-1}. Minithra et al [43] observed CH_2 asymmetric and symmetric stretching at 2982, 2932 cm^{-1} and 2905, 2893 cm^{-1} and assigned at 2978, 2930, 2885 cm^{-1} in the IR spectrum and at 2971, 2935, 2898 cm^{-1} in the Raman spectrum. For the title compound, the asymmetric CH_2 stretching calculated at 2970, 2922, 2910, 2872 by B3LYP/6-31G method and 2933, 2919, 2906, 2869 by B3LYP/6-31G(d,p) method. The symmetric CH_2 stretching observed at 2910 in FT-Raman spectrum and the computed values are 2915, 2896, 2841, 2830 by B3LYP/6-31G method and 2912, 2893, 2835, 2822 by B3LYP/6-31G(d,p) method. For the title compound, CH_2 scissoring band observed at 1394, rocking at 1173 in the IR spectrum and scissoring at 1415, 1400, rocking at 1200, wagging at 800 in the Raman spectrum. For the title compound, the CH_2 stretching modes are observed at σ_{sci} = 1429, 1423, 1408, 1402 cm^{-1}, ρ_{rock} = 1214, 1210, 1179, 1165 cm^{-1}, τ= 1118, 1110, 1056, 1044 cm^{-1}, $\delta_{wagg.}$ = 817, 805, 785, 775 cm^{-1} by B3LYP/6-31G, σ_{sci} = 1422, 1415, 1399, 1395 cm^{-1}, ρ_{rock} = 1207, 1200, 1175, 1163 cm^{-1}, τ= 1113, 1105, 1051, 1040 cm^{-1}, $\delta_{wagg.}$ = 812, 802, 780, 769 cm^{-1} by B3LYP/6-31G (d,p) methods respectively.

4.2.4 C-O vibrations

The C-O stretching vibrations [44, 37] are expected in the region 1715-1600 cm^{-1}. The in-plane deformation of C-O found in the region 625 ± 70 $cm^{-1}$and out-of-plane bending is in the range 540 ± 80 cm^{-1}[37].

Lucose et al [45] observedC-O stretching vibrations at 1632 cm^{-1} in IR spectrum and theoretically at 1636 cm^{-1} (DFT). In-plane bending at 569 cm^{-1} in IR and 555 cm^{-1} in DFT is assigned as this mode and out-of-plane bending at 673, 676 cm^{-1} in the IR spectrum.

The C=O stretching vibration appears both in the FT-IR and FT-Raman spectra due to intra molecular charge transfer from donor atom to acceptor atom through σ and π bonds conjugated path, which can induce large variation in dipole and molecular polarizability of the molecule and hence high activity in both spectra [37]. Renjith etal [34] observed the C-O modes at 1625 at IR and 1614, 1626 cm^{-1} at Ramanspectrum. The C-O stretching modes are reported at 1786, 1603, 1027 cm^{-1} and at 1726, 1629 cm^{-1} in the FT-IR, Raman spectrum and 1184, 1083, 1010, 974, 696 cm^{-1} assigned theoretically by Sakthivel et al [46]. Benzon et al [47] reported the C-O stretching mode at 1212 cm^{-1}

Annals of R.S.C.B., ISSN:1583-6258, Vol. 25, Issue 5, 2021, Pages. 1587 - 1628
Received 15 April 2021; Accepted 05 May 2021.

(IR), 1228 cm^{-1} (Raman) and at 1229 cm^{-1} theoretically. For the title molecule, C-O stretching vibrations observed at 1679, 1254 cm^{-1} in IR spectrum and 1680, 1295 cm^{-1} in Raman spectrum. The reported values for υC-O = 1683, 1301, 1260 cm^{-1}, δCO = 1346, 984, 965 cm^{-1}, γCO= 685, 630, 620 cm^{-1} by B3LYP/6-31G method, υC-O = 1680, 1297, 1254 cm^{-1}, δCO = 1342, 980, 963 cm^{-1}, γCO= 679, 626, 620 cm^{-1} by B3LYP/6-31G (d,p) methods respectively.

4.2.5 C-C vibrations

C-C stretching vibrations occur in the range of 1625-1465 cm^{-1} [48]. The in-plane and out-of plane bending modes of C-C were reported at 725± 95 and 595 ± 120 cm^{-1} [49].

The C-C band observed by Kuruvilla et al [26] at 1579, 1531, 1439, 1380, 1123 for FT-Raman and for FT-IR bands at 1428, 1235, 1002 cm^{-1}.Soleymani et.al [32] observed C-C band at 1625, 1590, 1575, 1540, 1470, 1465, 1430, 1380, 1280 cm^{-1}. Tamil elakkiya et al [36] observed the C-C band at 1313, 1039 cm^{-1} and calculated at 1600, 1625, 1319, 1054 cm^{-1}. In the present work, the C-C vibrations observed at 1591, 1230, 1118, 909 in IR spectrum, 1215, 910 in Raman spectrum. The reported values at 1644, 1625, 1613, 1596, 1538, 1236, 1221, 1195, 1186, 1162, 1145, 1140, 1131, 1125, 1080, 1013, 992, 925,924, 914, 845 cm^{-1} by B3LYP/6-31G method, 1641, 1623, 1604, 1590, 1533, 1231, 1217, 1191, 1182, 1158, 1143, 1136, 1127, 1120, 1075, 1009, 989, 921, 916, 910, 842 cm^{-1} by B3LYP/6-31G (d,p) methods respectively. The C-C in-plane bending observed at 503 and 502, 345 in IR and Raman spectrum and the reported values are 792, 715, 690, 616, 608, 590, 575, 565, 539, 510, 503, 477, 480, 360, 349 cm^{-1} by B3LYP/6-31G method,786, 711, 688, 612, 603, 586, 573, 561, 535, 506, 500, 472, 466, 354, 345 cm^{-1} by B3LYP/6-31G (d,p) methods. The C-C out-of-plane bending vibration assigned at 150, 135, 120 in Raman spectrum and the calculated values are at 330, 319, 303, 296, 291, 273, 262, 246, 197, 189, 176, 158, 141, 126 cm^{-1} by B3LYP/6-31G method, 325, 314, 299, 293, 286, 275, 268, 242, 191, 185, 173, 151,136, 120 cm^{-1} by B3LYP/6-31G (d,p) methods.

4.2.6 C-N vibrations

The CN stretching modes are expected in the region 1400-1200 cm^{-1}

Sandhyarani et al [50] reported the C-N stretching mode at 1319 cm^{-1}. Benzon et al [47] reported at 1247, 129, 938 cm^{-1} theoretically, 1268, 11135, 926 cm^{-1} in the Raman spectrum and 924 cm^{-1} in the IR spectrum. The C-N stretching modes were reported at 1268, 1220, 1151cm^{-1} theoretically by Malek

Annals of R.S.C.B., ISSN:1583-6258, Vol. 25, Issue 5, 2021, Pages. 1587 - 1628
Received 15 April 2021; Accepted 05 May 2021.

et.al [51]. Al-Alshaikh et.al.[52] observed C-N stretching mode at 1329, 1092, 997 cm^{-1} in the IR spectrum, 1328 cm^{-1} in the Raman spectrum and theoretically at 1479, 1472, 1331, 1097, 998 cm^{-1} . Bhagyasree et al [53] reported C-N stretching modes at 1247 and 1236 cm^{-1} and Mary et al [14] reported the C-N stretching modes at 1233, 1209 cm^{-1} by theoretically and 1238 cm^{-1} by Raman spectrum. shanaparveen et al [28] assigned the C-N stretching mode at 1579 cm^{-1} and IR spectrum at 1553 cm^{-1} . In the present work, C-N stretching vibrations observed at 1541 and 1350, 720 in IR and Raman spectrum. The predicted values at 1579, 1533, 1525, 1370, 1356, 726 and 1572, 1529, 1517, 1362, 1351, 720 cm^{-1} by B3LYP/6-31G and 6-31G(d,p) methods.

4.2.7 N-N vibrations

N-N stretching mode occurs at 1417-1372 cm^{-1}[54].The υN-N has been reported at 1151 cm^{-1} by Crane et al [55], 1121 $cm^{-1}$by Bezerra et al [56] and 1130 cm^{-1} El-behery and El-Twigry [57] and 1083 cm^{-1} theoretically by Sundaragensan et al [58]. Binil et al [59] reported the N-N stretching mode at 1138 cm^{-1} in IR, 1139 cm^{-1} in Raman and 1136 cm^{-1} theoretically. For Murugavel et al [40], N-N stretching vibrations allocated at 1083, 1119 cm^{-1} by DFT technique and experimentslly at 1082 cm^{-1} in FTIR spectrum. For the title molecule, N-N stretching mode is calculated at 883 and 879 cm^{-1} by B3LYP/6-31G and 6-31G(d,p) methods respectively.

4.2.8 C-S vibrations

This vibration cannot be identified easily as it results in weak infrared bands, which is susceptible to coupling effects and is also of variable intensity. In general, the C-S stretching vibration was reported in 750-600 cm^{-1} [60].

Benzon et al [27] reported value this mode at 1515 cm^{-1} in the IR spectrum, 1520 cm^{-1} in the Raman spectrum, 1517 cm^{-1} theoretically. The C-S stretching mode observed for Sarau et al [23] are assigned at 759, 660 cm^{-1} theoretically and experimentally observed at 756, 665 cm^{-1} and 756, 658 cm^{-1}in the IR and Raman spectrum. Kuruvilla etal [33] observed these vibrations at 822,608 cm^{-1} and theoretically at 714 cm^{-1}. The C-S stretching modes were observed by Coates [53] in the range 710-687cm^{-1} while Kwiastkowski et al [61] reported the vibration at 839 and 608 cm^{-1}. The C-S stretching vibrations are reported at 783, 632 cm^{-1} and 633 cm^{-1} IR, Raman spectrum and 785, 635 cm^{-1} theoretically found by El-Azab et al [62]. The C-S stretching vibrations are reported at 770 cm^{-1} in the

Annals of R.S.C.B., ISSN:1583-6258, Vol. 25, Issue 5, 2021, Pages. 1587 - 1628
Received 15 April 2021; Accepted 05 May 2021.

IR spectrum, and at 770, 636 cm^{-1} theoretically assigned by ShaheenFatma et al [48]. In the present work, C-S vibrations calculated at 738, 697 and 731, 694 cm^{-1} by B3LYP/6-31G and 6-31G(d,p) methods respectively.

4.2.9 C-Cl vibrations

The vibrations belong to C-Cl absorption is obtained in the region between 850-550 cm^{-1} [63].

Kuruvilla1 et al [26] observed theoretically at C-Cl vibration at 694 and 415 cm^{-1} and experimentally at 710-505 cm^{-1}. Jayasheela et al [35] reported this band at 725 and 720 cm^{-1} 4-chlorophenyl ({[(1E)-3-(1Himidazol-1-yl)-1-phenylpropylidene]amino}oxy) methanone for theoretically and experimentally. For the title compound, the vibrations occurs at for υC-Cl= 597, δ C-Cl=438 in FT-IR spectrum and theoretically at υC-Cl=602 and 598 cm^{-1}, δ C-Cl=473 and 440 cm^{-1}, γ C-Cl=280 and 275 cm^{-1} by B3LYP/6-31G and 6-31G(d,p) methods respectively.

4.2.10 Ring vibration

The thiazole ring in-plane bending vibrations are observed at 551, 457, 411 by FT-IR spectrum and theoretically at 588, 553, 545,531, 522, 487, 463, 427, 417, 407, 392,381, 166, 146, 112, 52, 48 cm^{-1} by B3LYP/6-31G method and 580, 550, 541, 523, 518, 481, 460, 422, 410, 401, 389, 375, 162, 142, 102, 49, 46, 43 cm^{-1} by B3LYP/6-31G(d,p) method. The ring out-of-plane bending observed at 35 in FT-Raman spectrum, theoretically at 135, 95, 86, 80, 75, 66, 41, 37,30, 25, 23, 17, 12, 7 cm^{-1} by B3LYP/6-31G method and 128, 89, 79, 74, 69, 57, 35, 30, 24, 22, 20, 16, 10, 6 cm^{-1} by B3LYP/6-31G(d,p) method.

4.3 Molecular electrostatic potential (MEP) surface analysis

Molecular electrostatic potential at a point in space around a molecule gives information about the net electrostatic effect produced at that point by total charge distribution (electron + proton) of the molecule and correlates with dipole moments, electro-negativity, partial charges and chemical reactivity of the molecules. It provides a visual method to understand the relative polarity of the molecule [64, 65]. An electron density iso-surface mapped with electrostatic potential surface depicts the size, shape, charge density and site of chemical reactivity of the molecules. Figure 4 illustrates the charge distributions of the molecule two dimensionally. As it can be seen from the figure, the different

Annals of R.S.C.B., ISSN:1583-6258, Vol. 25, Issue 5, 2021, Pages. 1587 - 1628
Received 15 April 2021; Accepted 05 May 2021.

values of the electrostatic potential at the surface are represented by different colours; red represents region of most electronegative electrostatic potential, blue represents region of the most positive electrostatic potential and green represents region of zero potential. Potential increases in the order red < orange < yellow < green < blue. Blue indicates the strongest attraction and red indicates the strongest repulsion. Region of negative potential are usually associated with the lone pair of electronegative atoms. As can be seen from the MEP map of the title molecule, more reactive sited are close to C=O (C40-O44) groups, the region having the most negative potential over oxygen atom O44 and O58, then all the hydrogen atoms have positive potential.The negative potential which is represented by red colour corresponds to an interaction of a proton by aggregate the electron density of the molecule represented by red yellow shade and blue region is positive which corresponds to the repulsion of the proton represented by blue shades.

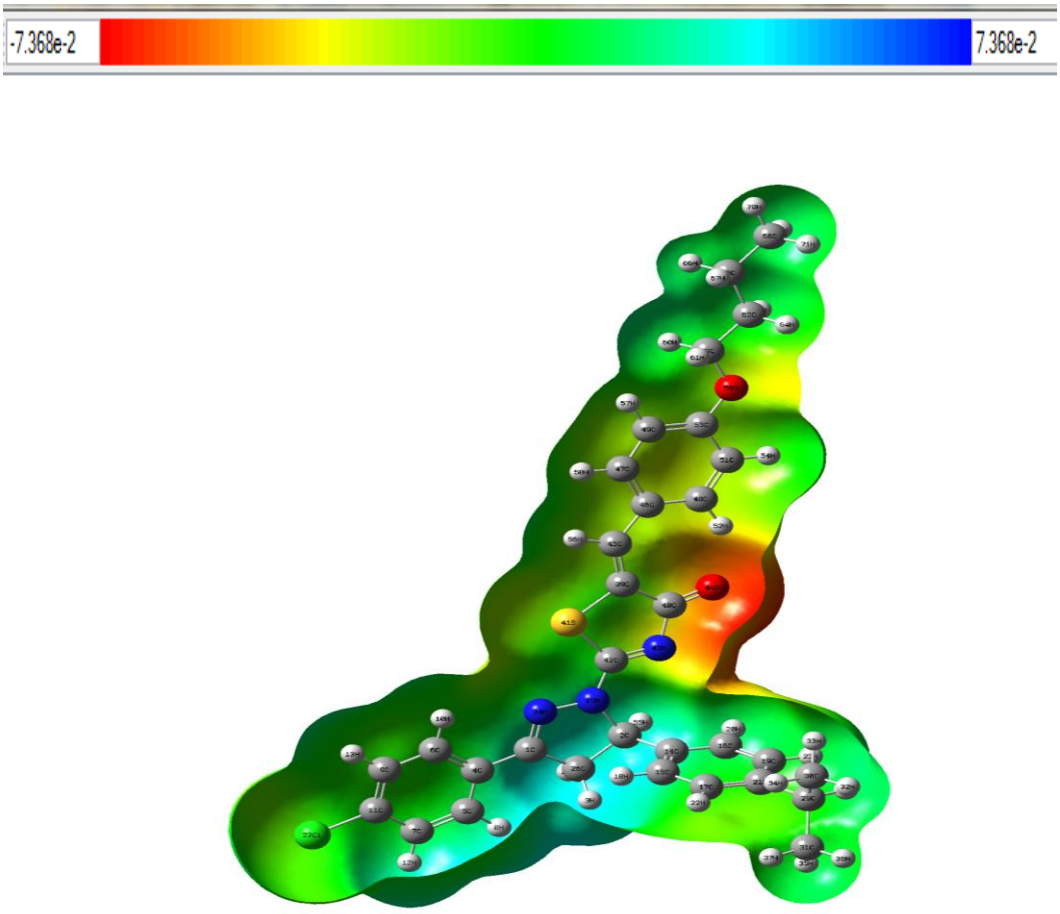

Figure 4: Molecular electrostatic potential surfaces of 5-(4-Butoxybenzylidene)-2-[3-(4-chlorophenyl)-5[4-(propan-2-yl)-4,5-dihydro-1H-pyrazol-1-yl]-1,3-thiazol-4(5H)-one

Annals of R.S.C.B., ISSN:1583-6258, Vol. 25, Issue 5, 2021, Pages. 1587 - 1628
Received 15 April 2021; Accepted 05 May 2021.

The strong negative region spread over the phenyl rings, nitrogen atom and oxygen atom of the hydroxyl group and these are possible sites of electrophilic sites. The positive electrostatic potential regions are fully covered all the hydrogen atoms and it represents the possible site of the nucleophilic sites in the MEP plot.

4.4Frontier molecular orbital (FMO) study

DFT method with 6/31G(d,p) basis set is applied to compute the energy of HOMO and LUMO levels and the energies are shown in Table 3. The Frontier molecular orbitals (FMO) play a significant function in the electric and quantum chemistry [66]. The pictorial demonstration of these different FMOs is shown in Figure 5. The HOMO is the donor and LUMO is acceptor orbital and the energy difference between HOMO and LUMO have been used to investigate the global reactivity descriptors. The electrophilic index (ω), hardness (η) and chemical potential (μ) are known reactivity parameters. These parameters are considered as highly successful descriptors for biological activity.Moreover, electronegativity (χ),electron affinity (A), ionization potential (I) are also determined using the energies of frontier molecular orbitals and these reactivity parameters used in understanding the site selectivity and the reactivity. The compounds that possess positive electron affinity are known as electron acceptors and might participate in charge transfer reactions. The electron donation strength for any donor compound can be measured using ionisation potential is the energy which need to take off an electron from the HOMO. Electronegativity is known as one for the most important chemical properties which defined as power of species to attract electrons towards itself. The large E_{HOMO}-E_{LUMO} differences define a hard species, which means compound is more stable and less reactive. While, small E_{HOMO}- E_{LUMO} gap defines a soft species is less stable and more reactive. The calculated energy of HOMO is -5.3304 eV and LUMO is -1.9783 eV and the energy gap for the title compound is 3.3521 eV and is a hard one. Ionization potential (I) =5.3304 eV, Electron affinity (A) = 1.9783 eV, Global hardness (η) = 1.6761 eV, Softness (η) = 0.5966 eV, Chemical potential (μ) = -3.6544 eV, Electrophilicity index (ω) = 3.9838 eV. The values for chemical potential and electrophilicity index are small that indicates the reactive nature of the title compound which confirms the bioactivity of the title molecule by the positive value of chemical softness.

Annals of R.S.C.B., ISSN:1583-6258, Vol. 25, Issue 5, 2021, Pages. 1587 - 1628
Received 15 April 2021; Accepted 05 May 2021.

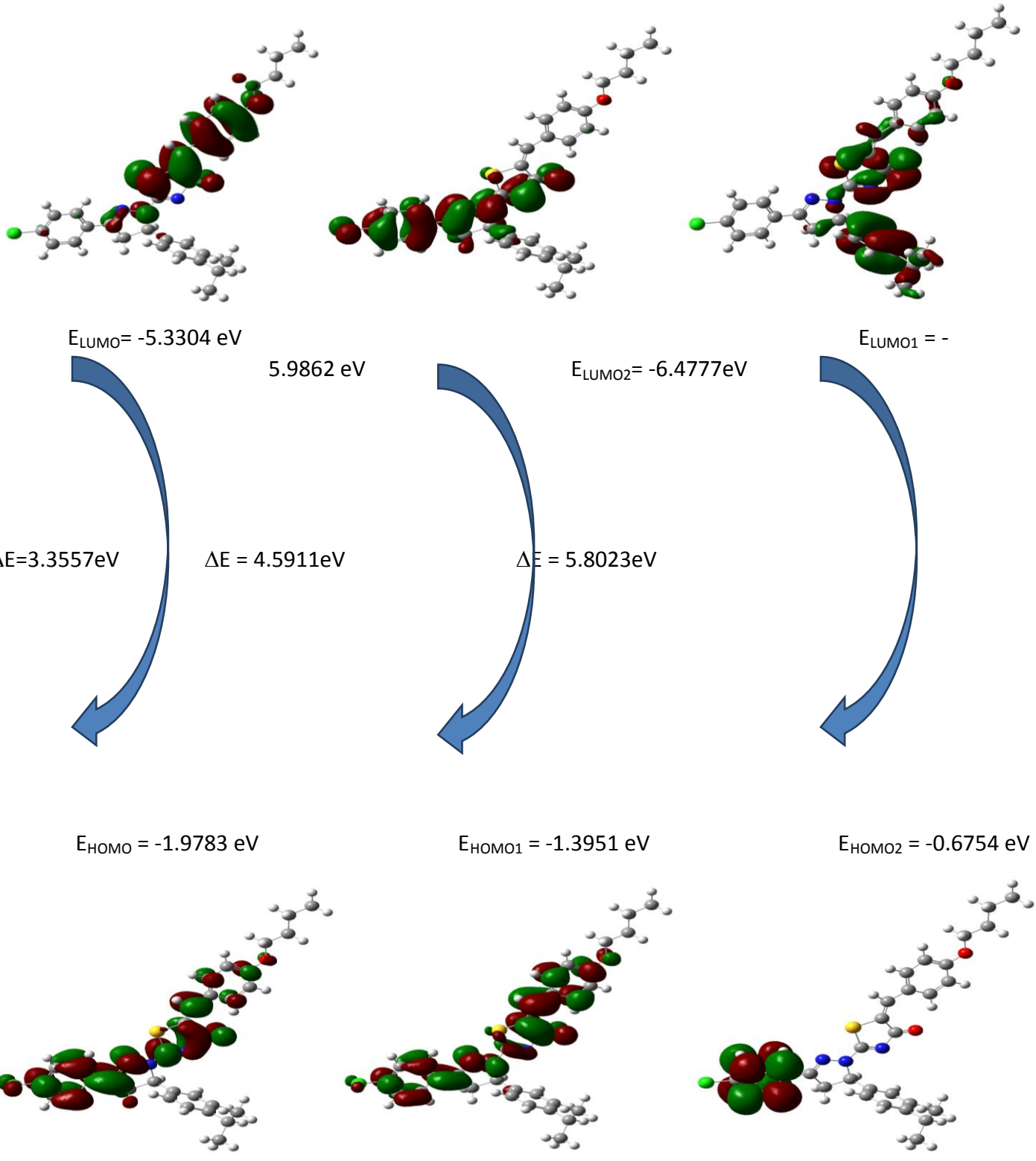

Annals of R.S.C.B., ISSN:1583-6258, Vol. 25, Issue 5, 2021, Pages. 1587 - 1628
Received 15 April 2021; Accepted 05 May 2021.

Figure 5:Patterns of the principle highest occupied and lowest unoccupied molecular orbital 5-(4-Butoxybenzylidene)-2-[3-(4-chlorophenyl)-5[4-(propan-2-yl)-4,5-dihydro-1H-pyrazol-1-yl]-1,3-thiazol-4(5H)-one

Table 3 HOMO-LUMO energies for 5-(4-Butoxybenzylidene)-2-[3-(4-chlorophenyl)-5[4-(propan-2-yl)-4,5-dihydro-1H-pyrazol-1-yl]-1,3-thiazol-4(5H)-one by B3LYP/6-31G (d,p) basis set

Molecular properties	Energy (eV)	Energy gap (eV)	Ionisation potential(I)	Electron affinity (A)	Global hardness (η)	Global softness (σ)	Chemical potensial (μ)	Global Electroplicity(ω)
E_{HOMO}	-5.3304							
E_{LUMO}	-1.9783	3.3521	5.3304	1.9783	1.6761	0.5966	-3.6544	3.9838
E_{HOMO-1}	-5.9862							
E_{LUMO-1}	-1.3951	4.5911	5.9862	1.3951	2.2955	0.4356	-3.6907	2.9669
E_{HOMO-2}	-6.4777							
E_{LUMO-2}	-0.6754	5.8023	6.4777	0.6754	2.9012	0.3447	-3.5765	2.2045

4.5 Reduced density gradient

RDG is a pictorial visualization of various kinds of non-covalent interactions directly in the real space using Multiwfn and plotted by visual molecular dynamics (VMD) program [20,21]. Noncovalent interactions are very weak when compared with covalent bonds and hence play a vital role in nature. To understand the nature of inter molecular interaction of the title compound, RDG analyses were carried out and the resultant graphs are shown in Figure 6.

Annals of R.S.C.B., ISSN:1583-6258, Vol. 25, Issue 5, 2021, Pages. 1587 - 1628
Received 15 April 2021; Accepted 05 May 2021.

According to this graph, the green regions represent weak attractive interactions (λ2≈0) such as Van der Waals interaction; strong attractions like H-bond, C-Cl bonds are represented by blue colour. The red colour represents steric repulsion appears in the inside of phenyl rings, pyrazole, and 4-Butoxybenzylidene while van der waals interactions took place near 4(propan-2-yl) and over hydrogen atoms. The negative values of λ(2)ρ indicates strong attractive interactions, while the positive values mean the repulsive interactions.

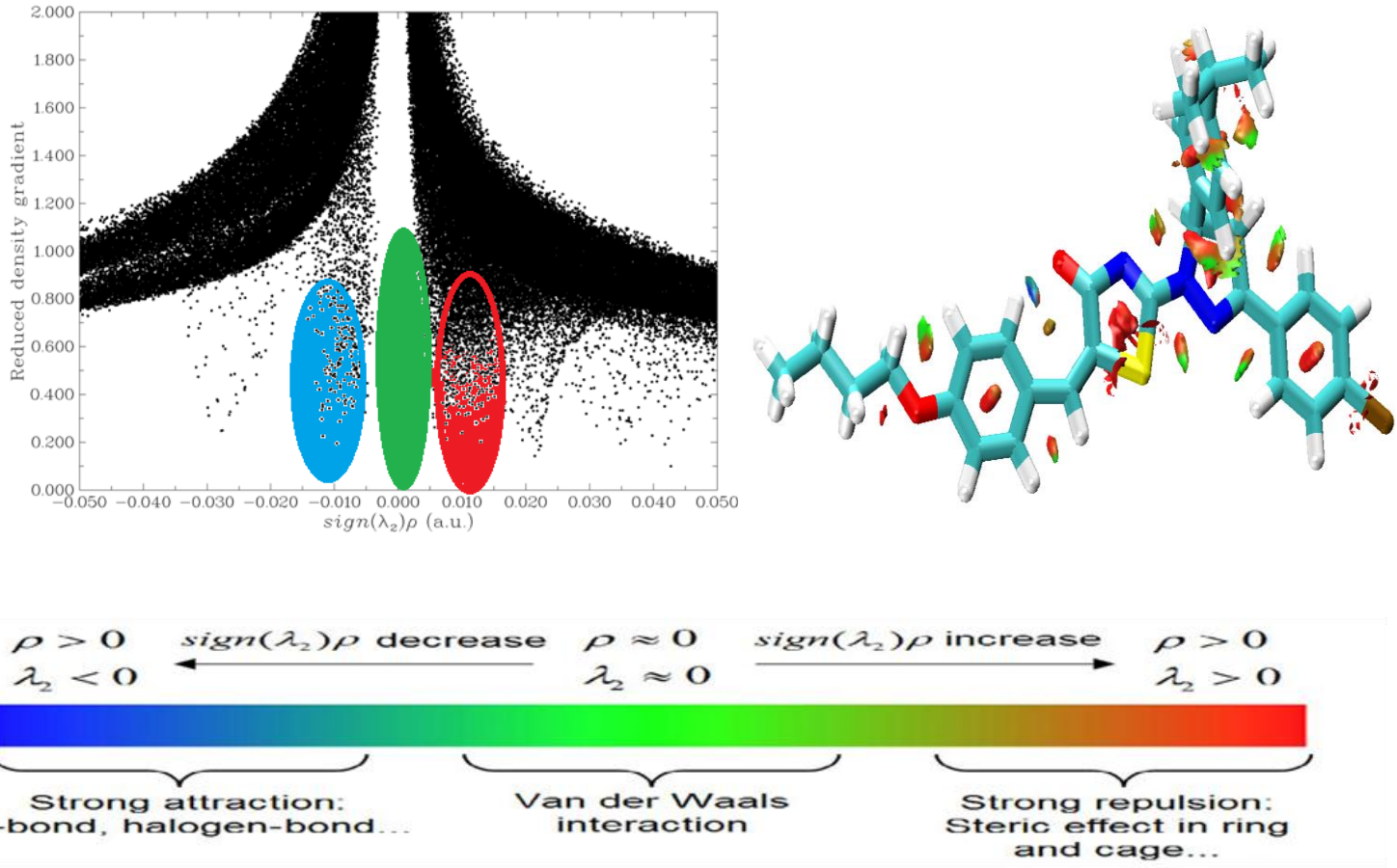

Figure 6:Plots of the RDG versus λ(2)ρ of 5-(4-Propan-2-yl)benzylidene)-2-[3-(4-chlorophenyl)-5[4-(propan-2-yl)phenyl-4,5-dihydro-1H-pyrazol-1-yl]-1,3-thiazol-4(5H)-one

4.6 Molecular docking

Molecular docking is a computer-assisted drug design (CADD) method used to predict the favourable orientation of a ligand (drug) to a target (receptor) when bound to each other to form a

Annals of R.S.C.B., ISSN:1583-6258, Vol. 25, Issue 5, 2021, Pages. 1587 - 1628
Received 15 April 2021; Accepted 05 May 2021.

stable complex. By understanding the favoured orientation can be used to find out the strength of binding affinity between ligand and target site, e.g. by docking score [67]. Moreover, docking study can be used to find out type of interactions between ligand and receptor like hydrogen bonding and hydrophobic interactions. Hence, molecular docking can be considered as first-line technique for a pharmaceutical lead discovery [68].Molecular docking studies were carried out to understand the binding profile of thiazole derivatives and to support the in vitro anticancerous activity. Automated docking was used to determine the orientation of inhibitors bound in the active site of Tubulin(PDB ID=4YJ2), which the protein has anti-cacerous activity. Protein 4YZJ has antiviral and 1OQE, 4YJE has anti tumer activity. A Lamarckian genetic algorithm method, implemented in the program AutoDockVina software was employed. The ligand used for docking was the optimized structure at B3LYP/6-31G (d, P). The files were prepared in a pdb format. The protein structure file (PDB ID: 4YZJ) taken from RCSB Protein Data Bank (PDB) was prepared for docking by removal of water molecules, adding polar hydrogens and Kollman charges to the structure file. In silico prediction of amino acids involved in the active site of protein responsible for binding with the ligands are obtained from the co-crystallized endogenous ligand from the PDB file. The ligand was docked in the functional sites of the selected protein and minimum docking energy value was examined. Docked conformation which had the lowest binding energy was chosen to scrutinize the molecule mode of binding. The molecular docking binding energies and inhibition constants were also obtained and listed in Table 4 The title compound taken as the ligand interactions with proteins are shown in Figure 7.

Annals of R.S.C.B., ISSN:1583-6258, Vol. 25, Issue 5, 2021, Pages. 1587 - 1628
Received 15 April 2021; Accepted 05 May 2021.

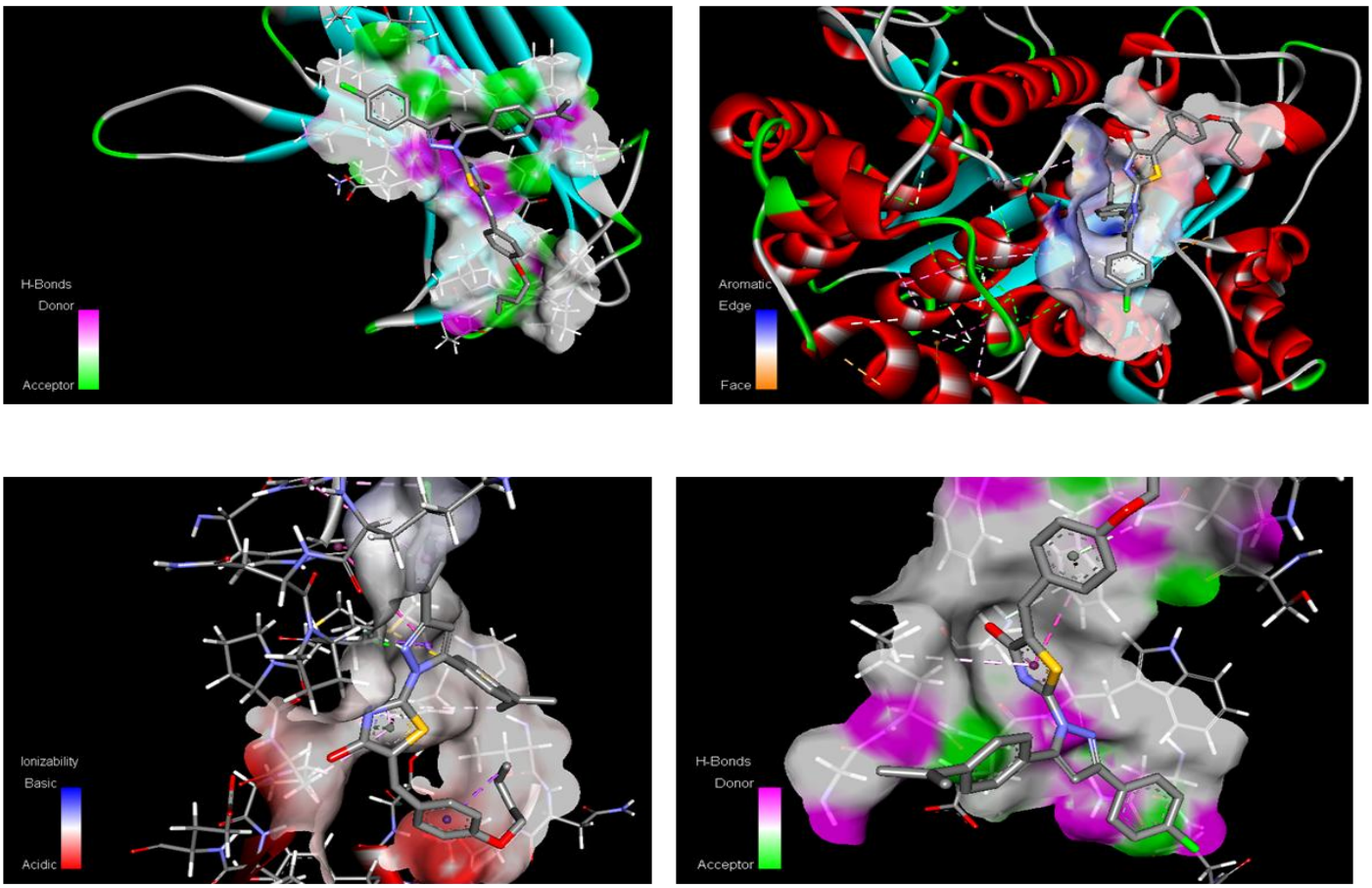

Figure 7:Ligand - 5-(4-Butoxybenzylidene)-2-[3-(4-chlorophenyl)-5[4-(propan-2-yl)-4,5-dihydro-1H-pyrazol-1-yl]-1,3-thiazol-4(5H)-one, Proteins – 1JH5,1OQE, 4YJ2 and 4JZJ

Table 4:Binding affinity for docking in5-(4-Butoxybenzylidene)-2-[3-(4-chlorophenyl)-5[4-(propan-2-yl)-4,5-dihydro-1H-pyrazol-1-yl]-1,3-thiazol-4(5H)-one

Drug	Protein	Type of activity	Binding affinity(kcal/mol)	Etimated inhibition constant Ki(µM)	Bonded residues	Nature of bond	Bond distance (Å)	RMSD
(4-chlorophenyl)-4-(propan-2-yl)-4-ydro--1H-pyrazol-1--thiazol-4(5H)-o			-4.7	360.43	ASN A-42	Conventional hydrogen bond	3.31	87.206
			-4.33	667.85	PRO A-15	Alkyl	4.1	71.635

Annals of R.S.C.B., ISSN:1583-6258, Vol. 25, Issue 5, 2021, Pages. 1587 - 1628
Received 15 April 2021; Accepted 05 May 2021.

	1OQE	Antitumer	-4.19	845.86	ILE A-15	Alkyl	4.17	78.414
			-3.97	1.23(mM)	GLU A-41	Conventional hydrogen bond	4.32	81.106
			-3.8	1.64 (mM)	ASN A-42	Conventional hydrogen bond	4.55	82.083
	4YJ2	Anticancer	-4.7	358.4	LEU A-397	Alkyl	3.72	80.983
			-4.6	426.72	PRO A-175	Alkyl	3.82	121.029
			-4.21	817.23	PRO A-173	π-alkyl	4.24	111.228
			-4.57	447.01	PRO A-184	π-alkyl	4.39	87.283
			-4.53	482.07	GLN A-176	Carbon hydrogen bond	4.55	94.627
	4YJE	Antitumer	-5.42	106.41	MET A-438	Conventional hydrogen bond	3.64	49.944
			-5.42	106.79	MET A-438	Conventional hydrogen bond	3.8	47.995
			-5.32	126.67	TYR A-486	carbon hydrogen bond	3.89	48.812
			-5.2	155.59	MET A-438	Conventional hydrogen bond	4.02	33.732
			-4.95	234.91	MET A-438	Conventional hydrogen bond	4.17	25.064
	4JZJ	Antiviral	-5.17	163.56	PHE A: 107	van der waals	3.85	36.106
			-4.95	236.07	TRP A: 47	van der waals	4.65	36.427
			-4.49	514.73	PHE A:	van der waals	4.94	30.37

Annals of R.S.C.B., ISSN:1583-6258, Vol. 25, Issue 5, 2021, Pages. 1587 - 1628
Received 15 April 2021; Accepted 05 May 2021.

					107			4
			-4.23	790.86	TRP A: 106	π-π Stacked	5.05	38.123
			-4.2	838.87	LEU A: 45	π-π Stacked	5.08	32.471

4.6.1 Anti-tumer activity

Interaction of antitumor protein 1OQE shows the existence of many conventional bonds such as three conventional hydrogen bonds and two alkyl bond interaction with amino acid (ASN A: 42, GLU A: 41, ASN A: 42, PRO A: 15, ILE A: 15) with different binding energies (-4.7, -3.97, -3.8, -4.33, -4.19)kcal/mol, inhibition constants (360.43, 1.23 (mM), 1.54 (mM), 667.85, 845.86)ki(μM) RMSD values are (87.206, 81.106, 82.083, 71.635, 78.414)Å. Interaction of antitumor protein 4YJE shows the existence of many conventional bonds such as five conventional hydrogen bond interaction with amino acid (MET A: 438, MET A: 438, TYR A: 486, MET A: 438, MET A: 438) with different binding energies (-5.42, -5.32, -5.2, -4.95, -4.45)kcal/mol, inhibition constants (106.41, 126.67, 155.59, 234.91, 544.29)ki(μM) RMSD values are (49.944, 48.812, 33.732, 25.064, 25.158)Å.

4.6.2 Anticancer activity

Interaction of anticancerous protein 4YJ2 shows the existence of many conventional bonds such as one Alkyl bonds, two π-alkyl bond and one carbon hydrogen bond interaction with amino acid (LEU A: 397, PRO A: 175, PRO A: 173, PRO A: 184, GLN A: 176) with different binding energies (-4.7, -4.6, -4.21, -4.57, -4.53)kcal/mol, inhibition constants (358.4, 426.72, 817.23, 447.01, 482.07)ki(μM) RMSD values are (80.983, 121.029, 111.228, 87.283, 94.627)Å.

4.6.3 Antiviral activity

Interaction of antiviral protein 4JZJ shows the existence of many conventional bonds such as three van der waals bonds and two π-π stackedbond interaction with amino acid (PHE A: 107, TRP A: 47, PHE A: 107, TRP A: 105, LEU A: 45) with different binding energies (-5.17, -4.95, -4.49, -4.23, -

4.2)kcal/mol, inhibition constants (163.56, 236.07, 514.73, 790.86, 838.87)ki(μM) RMSD values are (36.106, 36.427, 30.374, 38.123, 32.471)Å.

5. Conclusion

Structures of the title compounds were investigated using high-level quantum chemistry calculation. The optimized geometrical parameters and vibrational frequency assignment of the fundamental modes of title compounds have been obtained from DFT/B3LYP/6-31G and DFT/B3LYP/6-31G(d, p) level of calculation. The HOMO and LUMO analysis are used to determine the charge transfer within the molecule and the calculated HOMO and LUMO energies show the chemical activity of the molecule. The energy gap of the title molecule is ΔE= 3.3557eV. From the molecular electrostatic potential plot, it is evident that the negative charge covers the carbonyl group and the positive region is over the remaining groups and the more electronegativity in the carbonyl group makes it the most reactive part of the molecule. Weak interaction profile shows that the presence of Van der Waals interactions and steric effect are present in the molecule. Molecular docking analysis reveals that the title molecule can act as a good inhibitor against the proteins 1JH5, 1OQE, 4YJ2 and 4JZJ.

Reference

[1] C. Hansch, P. G. Sammes, J. B. Taylor, “in: Comprehensive Medicinal Chemistry”, vol.2, Pergomen Press, Oxford, UK, 1990, (chapter 7) pp.1.
[2] M. D. MeReynolds, J. M. Dougerty, P. R. Hanson, “synthesis of phosphorus and sulfurheterocycles via ring-closing metathesis”, Chem. Rev. vol. 104 2004, pp.2239-2258.
[3] J. R. Lewis, “Amaryllidanceae, Sceletium, muscarine, imidazole, oxazole, peptide and other miscellaneous alkaloids”,Nat. Prod. Rep. vol. 16 1999,pp.389-416.
[4] R. J. Nevagi, “Biological and medical significance of 2-Aminothiazoles”, Der.Pharm.Lett. vol. 6, 2014,pp. 134-150.
[5] M. H. M. Helal, M. A. Salem, M. S. A. El-Gaby, M. Aljahdali, “Synthesis and biological evalution of some novel thiazole compounds as potential anti-inflammatory agents”, Eur.J.Med .Chem. vol. 65, 2013, pp. 517-526.
[6] F. Haviv, J. D. Ratajczyk, R. W. DeNet, F. A. Kerdesky, R. L. Walters, S. P. Schmidt, J. H. Holms, P. R. Young, G. W. Carter, “3-[1-(2-enzoxazolyl)hydrazine]propanenitrile derivatives: inhibitors of immune complex induced inflammation”, J.Med.Chem. vol. 31, 1988,pp. 1719-1728;

[7] K. D. Hargrave, F. K. Hess, J. T. Oliver, "N-(4-substituted-thiazolyl)oxamic acid derivatives, a new series of potent , orally active antiallergy agents", J.Med.Chem.,vol. 26, 1983, pp. 1158-1163.
[8] M. Grimstrup, F. Zaragoza, "Solid-phase synthesis of 2-Amino-5-sulfanythiazoles", Eur.J.Org.Chem., 2002,pp. 2953-2960.
[9] J. C. Jean, L. D. Wise, B. W. Caprathe, H. Tecle, S. Bergmeier, C. C. Humblet, T. G. Heffner, L. T. Meltzner, T. A. Pugsley, "4-(1,2,5,6-Tetrahydro-1-alkyl-3-pyridinyl)-2-thiazolamines: a novel class of compounds with central dopamine agonist properties", J.Med.Chem. vol. 33, 1990,pp. 311-317.
[10] S. Annadurai, R. Martinez, D. J. Canny, T. Eidem, P. M. Dunman, M. A. Gharbia, "Design and synthesis of 2-Aminothiazole based antimicrobials targeting MRSA", Bioorg. Med Chem.Lett.,vol. 22, 2012 pp. 7719-7725.
[11] K. V. Sashidhara, K. B. Rao, V. Kushwaha, R. K. Modukuri, R. Verma, P. K. Murthy, "synthesis and antifilarialactivityofchlocone-thiazole derivatives against a human lymphatic filarial parasite, Brugiamalayi", Eur.L.Chem., vol. 81, 2014, pp. 473-480.
[12] S. E. Kazzouli, S. B. Rabin, A. Mouadbib, G. Guillaumet, "Solid support synthesis of 2,4-disubstituted thizoles and aminothiazoles", Tetrahedron Lett.,vol. 43, 2002, pp. 3193-3196.
[13] V. V. Salian, B. Narayana, B. K. Sarojini, M. S. Kumar, K. Sharath Chandra, A. G. Lobo, "Tailor made biheterocyclicpyrazoline-thiazolidinones as effective inhibitors of Escherichia coli FabH: design, synthesis and structural studies", Journal of Molecular Structure,vol. 1192, 2019, pp. 91-104.
[14] V. V. Salian, B. Narayana, B. K. Sarojini, E. S. Sindhupriya, L. N. Madhu, S. Rao, "Biologically potent pyrazoline derivatives from versatile (2)-1-(4-chlorophenyl)-3-[4-(propan-2-yl)phenyl]prop-2-en-1-one", Lett. Drug Des.Discov.,vol. 14, 2017, pp. 216-227.
[15] B. Narayana,V. V. Salian,B. K. Sarojini, J. P. Jasinski, "(2E)-1-(4-Chlorophenyl)-3-[4-(propan-2-yl)phenyl]prop-2-en-1-one", ActaCryst., vol. 70, 2014, pp. 855.
[16] M. J. Frisch, G. W. Trucks, H. B. Schlegel, G. E. Scuseria,M. A. Robb, J. R. Cheeseman, G. Scalmani, V. Barone, B. Mennucci, G. A. Peterson, H. Nakatsuji, M. Caricato, X. Li, H. P. Hratchain, F. Izmaylov, J. Bloino, G. Zheng, J. I. Sonnenberg, M. Hada, M. Ehara, K. Toyota, R. Fukuda, J. Hasegawa, M. Ishida, T. Nakajima, Y. Honda, O. Kitao, H. Nagari, T. Vreven, T. A. Montgomery Jr., J. E. Peralta, F. Ogliaro, M.Bearpark, J. J. Heyd, .Brothers E,Kudin K N, V. N. Staroverov, R. K. Kobayashi, J. Normand, K. Ragavachari, A. Rendell, J. C. Burant, S. S.B Iyengar, J. Tomasi, M. Cossi, N. Rega, J. M. Millam, M. Klene, J. E. Knox, J. B. Cross, V. Bakken, C. Adamo, J. Jaramillo, R. G. Gomperts, R. E. Strarmann, O. Yazyev, A. J. Austin, R. Cammi, C. Pomelli, J. W. Ochterski, R. I. Martin, K. Morokuma, V. G. Zakrzewski, G. A. Voth, P. Salvador, J. J. Dannenberg, S. Dapprich, O. Farkas, J. V. Ortiz, J. Cioslowski, D. J. Fox Gaussian, Inc., Wallingford CT,2009.

[17] A. A. C. Braga, N. H. Morgon, G. Ujaque, F. Maseras, "Computational characterization of the role of the base in the Suzuki-Miyaura cross-coupling reaction", J.Am.Chem.Soc., vol. 127, 2005, pp. 9298-9307
[18] A. A. V. Braga, G. Ujaque, F. Maseras, "A DFT study of full catalytic cycle of the Suzuki-Miyaura cross-coupling on a model system", organometallics.,vol. 34, 2006,pp. 3647-3658.
[19] R. Dennington, T. Keith, J. Millam, "Gauss view, Version 5", Semichem Inc., ShawneeMission, KS, 2009.
[20] T. Lu, F. Chen, "Multiwfn: a multifunctional wave function analyzer", J. Chem. Inf. Comput. Chem.,vol. 33, 2012,pp. 580-592.
[21] W. Humpheney, A. Dalke, K. Schulten, "VMD: Visual molecular dynamics", J. Mol. Graph.,vol. 14, 1996,pp. 33-38.
[22] G. M. Morris, D. S. Goodsell, R. S. Halliday, R. Huey, W. E. Hart, R. K. Belew, A. J. Olson, "Automated Docking Using a Lamarckian Genetic Algorithm and Empirical Binding Free Energy Function", J. Comput. Chem.,vol. 19, 1998,pp. 1639-1662.
[23] Y. S. Mary, K. Raju, I. Yildiz, O.Temiz-Arpaci, H. I. S. Nogueira, C. M. Granadeiro, C. Van Alsenoy, "FT-IR, FT-Raman, SERS and computational study of 5-ethylsulphonyl-2-(o-chlorobenzyl)benzoxazole", Spectrochim. Acta A: Molecular and Biomolecular Spectroscopy,vol. 96, 2012, pp. 617-625.
[24] S.S. Parveen, M.A. Al-Alshaikh, C.Y.Panicker,A. A. El-Emam, M. Arisoy, O. TemizArpaci, C. Van Alsenoy, "Synthesis, vibrational spectroscopic investigations, molecular docking, antibacterial and antimicrobial studies of 5-ethylsulphonyl-2-(p-aminophenyl)benzoxazole", Journal of Molecular Structure,vol. 1115, 2016,pp. 94-104.
[25] Y.S. Mary, N.R. El-Brollosy, A. A. El-Emam, O.A. Al-Deeb, P.J. Jojo, C.Y. Panicker,C. Van Alsenoy, "Vibrational spectra, NBO analysis, HOMO-LUMO and first hyperpolarizability of 2-{[(2-Methylprop-2-en-1-yl)oxy]methyl}-6-phenyl-2,3,4,5-tetrahydro-1,2,4-triazine-3,5-dione, a potential chemotherapeutic agent based on density functional theory calculations", Spectrochim. Acta A: Molecular and Biomolecular Spectroscopy,vol.133, 2014,pp.449-456.
[26] Tintu K. Kuruvilla, S. Muthu, Johanan Christian Prasana, Jacob George, S. Sevvanthi, "Spectroscopic (FT-IR, FT-Raman), quantum mechanical and docking studies on methyl[(3S)-3-(naphthalen-1-yloxy)-3-(thiophen-2-yl)propyl]amine", Journal of Molecular structure, vol. 1175, 2019,pp. 163-174.
[27] Tintu K. Kuruvilla, Johanan Christian Prasana, S. Muthu, Jacob George, "Quantum Mechanical Calculations and Spectroscopic (FT-IR, FT Raman) Investigation on 1-cyclohexyl-1-phenyl-3-(piperidin-1-yl)propan-1-ol, by density functional method", Int. J. Mater. Sci.,vol.12, 2017, pp. 282-301.
[28] S. Shana Parveen, A. Monirah Al-Alshaikh, C. YohannanPanicker, Ali A. El-Emam, Mustafa Arisoy, OzlemTemiz-Arpaci, C. Van Alsenoy, "Synthesis, vibrational spectroscopic investigations, molecular docking, antibacterial and antimicrobial studies of 5-ethylsulphonyl-2-(p-aminophenyl)benzoxazole" –Journal of Molecular Structure., vol.1115, 2016,pp.94-104.

[29] S. George, "Infrared and Raman Characteristic Group Frequencies e Tables and Charts", third ed., Wiley, Chichester, 2001.
[30] M. Silverstein, G. GlaytonBasseler, C. Morrill, "Spectrometric Identification of Organic Compounds", Wiley, New York, 1991.
[31] M. Arirazhagan, J. Senthil Kumar, "Vibrational analysis of 4-amino pyrazole (3,4-d)pyrimidine A joint FTIR, Laser Raman and scaled quantum mechanical studies", Spectrochim. Acta A: Molecular and Biomolecular Spectroscopy,vol. 82, 2011,pp.228-234.
[32] Reza soleymani, Yasin Mohammad salehi, Taherehyousofzad, Maryam karimicheshmehali, "Synthesis, NMR, Vibrational and Mass Spectroscopy with DFT/HF Studies of 4-(4/-Bromophenyl) -2Mercaptothiazole Structure", Oriental journal of chemistry,vol.28, 2012,pp.627-638.
[33] A. Sarau Devi, V.V. Aswathy, Y. Sheena Mary, C. YohannanPanicker, StevanArmaković, J. Sanja. Armaković, ReenaRavindran, C. Van Alsenoy, "Synthesis, XRD single crystal structure analysis, vibrational spectral analysis, molecular dynamics and molecular docking studies of 2-(3-methoxy-4-hydroxyphenyl) benzothiazole", Journal of Molecular Structure, vol.1148, 2017, pp.282-292.
[34] RenjithRaveendranPillai, Vidya V. Menon, Y. Shyma Mary, StevanArmakovi, Sanja J. Armakovi, C. YohannanPanicker, "Vibrational spectroscopic investigations, molecular dynamic simulations and molecular docking studies of N'-diphenylmethylidene-5-methyl-1H-pyrazole-3-carbohydrazide", Journal of Molecular Structure, vol.1130, 2017,pp. 208-222.
[35] K. Jayasheela, H. Lamya, AlWahaibi, S.Periyandi, Hanan M Hassan, S.Sebastian, S. Xavier, Joseph C.Daniel, Ali A. El-Emam, Mohamed I Attia – "Probing vibrational activities, electronic properties, moleculardocking and Hirshfeld surfaces analysis of 4-chlorophenyl({[1E)-3-(1H-imidazole-1yl)-1-phenylpropylidene]amino}oxy)methanone: A promising anti-candida agent", Journal of Molecular Structure,vol.1159, 2018,pp.83-95.
[36] M. Tamil Elakkiya, S. PremKumar, M. Sathiyendran, P. Suresh, V. Shanmugaiah, K. Anitha, "Structural, spectral, computational, thermal and antibacterial studies on a cocrystal: 2-aminopyrazine phthalic acid", Journal of Molecular Structure,vol.1173, 2018,pp. 635-646.
[37] N. P. G. Roeges, "A guide to the complete interpretation to IR spectra of organic compounds", Wiley, New York, 1994.
[38] B. Smith, "Infrared Spectral Interpretation. A Systematic Approach", CRC Press, Washington, DC, 1999.
[39]C. YohannanPanicker, HemaTresaVarghes, P.S. Manjula, B.K. Sarojini, B. Narayana, JaveedAhamad War, S.K. Srivastava, C. Van Alsenoy, Abdulaziz A. Al-Saadi, "FT-IR, HOMO–LUMO, NBO, MEP analysis and molecular docking study of 3-Methyl-4-{(E)-[4-(methylsulfanyl)-benzylidene]amino}1H-1,2,4-triazole-5(4H)-thione", Spectrochim. Acta, Molecular and Biomolecular Spectroscopy,vol.151, 2015,pp.198-207.

[40]**S.** Murugavel, C. Ravikumar, G. Jaabil, PonnusamyAlagusundaram, "Synthesis, crystal structure analysis, spectral investigations (NMR, FT-IR, UV), DFT calculations, ADMET studies, molecular docking and anticancer activity of 2-(1-benzyl-5-methyl-1H-1,2,3-triazol-4-yl)-4-(2-chlorophenyl)-6-methoxypyridine – A novel potent human topoisomerase IIα inhibitor", vol.1176, 2019, pp. 729-742.
[41] A. TherasaAlphonsa, C. Loganathan, S. Athavan Alias Anand, S.Kabilan, "Molecular structure, NMR, UV-Visible, Vibrational spectroscopic and HOMO, LUMO analysis of (E)-1-(2, 6-bis (4-methoxyphenyl)-3, 3-dimethylpiperidine-4-ylidene)-2-(3-(3, 5-dimethyl-1H-pyrazol-1-yl) pyrazin-2-yl) hydrazine by DFT method", Journal of Molecular Structure,vol. 1106, 2016, pp. 277-285.
[42] N.B. Colthup, L.H. Daly, S.E. Wilberly, "Introduction to IR and Raman spectroscopy", Academic press, NewYork 1990.
[43] R. Minitha, Y. Sheenamary, HemaTresa Varghese, YohannanPanikers, ReenaRavindran, K. Raju, V. Manikandan Nair, "FT-IR, FT-Raman, and computational study of 1H-2,2-dimethyl3H-phenothiazin-4[10H]-one", Journal of Molecular Structure, vol. 985, 2011,pp. 316-322.
[44] M. Barthes, G. De Nunzio, G. Ribet, "Polarons or proton transfer in chains of peptide", Synth.Met.Vol.76, 1996,pp. 337-340.
[45] JiluLukose, C. YohannanPanicker, Prakash S. Nayak, B. Narayana, B.K. Sarojini, C. Van Alsenoy, Abdulaziz A. Al-Saadi, "Synthesis, structural and vibrational investigation on 2-Phenyl-N-(pyrazin-2-yl)acetamide combining XRD diffraction, FT-IR and NMR spectroscopies with DFT calculations",SpectrochimicaActa Part A: Molecular and Biomolecular Spectroscopy, vol. 135, 2015, pp. 608-616
[46] S. Sakthivel, T. Alagesan, S. Muthu, Christina Susan Abraham, E. Geetha, "Quantum mechanical, spectroscopic study (FT-IR and FT - Raman), NBO analysis, HOMO-LUMO, first order hyperpolarizability and docking studies of a non-steroidal anti-inflammatory compound",Journal of Molecular Structure, vol. 1156, 2018, pp. 645-656.
[47] K.B. Benzon, HemaTresa Varghese, C. YohannanPanicker, KiranPradhan, Bipransh Kumar Tiwary, Ashis Kumar Nanda, C. Van Alsenoy, "Spectroscopic investigation (FT-IR and FT-Raman), vibrational assignments, HOMO-LUMO, NBO, MEP analysis and molecular docking study of 2-(4-hydroxyphenyl)-4,5-dimethyl-1H-imidazole 3-oxide",SpectrochimicaActa Part A: Molecular and Biomolecular Spectroscopy, vol. 146, 2015, pp. 307-322.

[48] ShaheenFatma, AbhaBishnoi, Vineeta Singh, Fatmah A.M. Al-Omary, Ali A. El-Emam, ShilendraPathak, RuchiSrivastava, Onkar Prasad, LeenaSinha, "Spectroscopic and electronic structure calculation of a potential antibacterial agent incorporating pyrido-dipyrimidine-dione moiety using first principles",Journal of Molecular Structure,vol.1110, 2016,pp.128-137.
[49] L.J. Bellamy,"The Infrared Spectrum of Complex Molecules", third ed., Chapman and Hall, London, 1975.

[50] N. Sandhyarani, G. Skanth, S. Berchmanns, V. Yegnaraman,T. Pradeep,"A combined surface-enhanced raman-x-ray photoelectron spectroscopic study of 2-mercaptobenzothiazole monolayers on polycrystalline Au and Ag films", Journal of Colloid Interface Sci., vol.209, 1999,pp. 154-161.
[51] K. Malek, A. Puc, G. Schroeder, V.I. Rybachenko, L.M. Proniewich, "FT-IR and FT-Raman spectroscopies and DFT modelling of benzimidazolium salts", Chem. Phys. Vol. 327, 2006,pp. 439-451.
[52] A. Monirah, Al-Alshaikh, Y. Sheena mary, C. Yohannanpaniker, Mohamed I. Attia, Ali A. El-Emam, C. Van Alsenoy, "Spectroscopic investigations and molecular docking study of 3-(1H-imidazole-1-yl)-1-phenylpropan-1-one, a potential precursor to bioactive agents", Journal of Molecular Structure,vol. 1109, 2016,pp. 131-138.
[53] J. B. Bhagyasree, J. Samuel, H.T. Varghese, C.Y. Panicker, M. Arisoy, O. Temiz-Arpaci, "Synthesis, FT-IR investigation and computational study of 5-[(4-bromophenyl)acetamido]-2-(4-tert-butylphenyl) benzoxale", Spectrochim. Acta, Molecular and Biomolecular spectroscopy, vol. 115, 2013,pp. 79-91.
[54] W.C. Harris, L.B. Knight, R.W. McNamee, J.R. Durig, "Vibrational spectra and structure of tetramethyltetrazine", Inorg. Chem.,vol.13, 1974,pp. 2297-2301.
[55] L.G. Crane, D. Wang, L.M. Sears, B. Heyns, K. Carron, "SERS surfaces modified with a 4-(2-pyridylazo)resorcinol disulfide derivative: detection of copper, lead and cadmium", Anal. Chem. 67 (1995) 360-364.
[56] A. C. S. Bezerra, Eduardo L De Sa, F.C. Nart, "In situ vibrational study of the intial steps during urea electrochemical oxidation", Journal of Physics and Chemistry.,vol. 101, 1997,pp. 6443-6449.
[57] M. El-Behery, H. El-Twigry, "Synthesis, magnetic, spectral and antimicrobial studies of Cu(II), Ni(II), Co(II), Fe(II) and UO_2(II) complexes of a new Schiff base hydrazone derived from 7-chloro-4-hydrazinoquinoline",Spectrochim. Acta Part A:, Molecular and Biomolecular spectroscopy, vol. 66, 2007,pp. 28-36.
[58] N. Sundaraganesan, S. Ayyappan, H. Umamaheswari, B.D. Joshua, "FTIR, FT-Raman spectra and ab initio, DFT vibrational analysis of 2,4-dinitrophenylhydrazine", Spectrochim. Acta,vol.66, 2007,pp. 17-27.
[59] P.S. Binil, Y.S. Mary, H.T. Varghese, C.Y. Panicker, M.R. Anoop, T.K. Manojkumar, "Infrared and Raman spectroscopic analyses and theoretical computation of 4-butyl-1-(4-hdroxyphenyl)-2-phenyl-3,5-pyrazolidinedione", SpectrochimicaActa Part A: Molecular and Biomolecular Spectroscopy, vol.94, 2012,pp. 101-109.
[60] J. Coates, "Interpretation of Infrared Spectra of Organic Structures", John Wiley, New York, 2000.
[61] J.S. Kwiatkowski, J. Leszczynski, I.Teca, "Molecular structure and infrared spectra of furan, thiophene, selenophene and their 2,5-N and 3,4-N derivatives: density functional theory and

conventional post-Hartree-Fock MP2 studies", Journal of molecular structure, vol.436, 1997,pp.451-480.
[62] S. Adel. El-Azab, K. Jalaja, Alaa A.-M. Abdel-Aziz, M. Abdulrahman, Al-Obaid,Y. Sheena Mary, C. YohannanPanicker, C. Van Alsenoy, "Spectroscopic analysis (FT-IR, FT-Raman and NMR) and molecular docking study of ethyl 2-(4-oxo-3-phenethyl-3,4dihydroquinazolin-2-ylthio)-acetate", Journal of Molecular Structure,vol.1119, 2016, pp. 451-461.
[63] E.F. Mooney, "The infra-red spectra of chloro- and bromobenzenederivativesII. Nitrobenzenes", Spectrochim. Acta,vol. 20, 1964,pp. 1021-1032.
[64] S. Chidangil, M.K. Shukla, P.C. Mishra, "A molecular electrostatic peotential mapping study of some Fluroquinolone anti-bacterial agents", J. Mol. Modeling annual, 1998,pp. 250-258.
[65] F.JavierLuque, J.M. Lopez, M. Orozco, Perspective on "Electrostatic interactions of a solute with a continuum. A direct utilization of ab initio molecular potentials for the prevision of solvent effects", Theor.Chem. Acc. Vol. 103, 2000,pp.343-345.
[66] I.Fleming, "Frontier Orbitals, Organic chemical Reactions", Wiley, London, 1976.
[67] B.K. Sarojini, B.G. Krishna, C.G. Darshanraj,B.R. Bharath, H. Manjunatha. "Synthesis, characterization, in vitro and molecular docking studies of new 2,5-dichloro thienyl substituted thiazole derivatives for antimicrobial properties". Eur J Med Chem, vol. 45, 2010,pp.3490-3496.
[68] B.K. Shoichet, S.L. McGovern, B. Wei, J.J. Irwin."Lead discovery using molecular docking", CurrOpinChem Bio, vol.6, 2002,pp. 439–446.